

Topological charge pumping in excitonic insulators

Zhiyuan Sun¹ and Andrew J. Millis^{1,2}

¹*Department of Physics, Columbia University, 538 West 120th Street, New York, New York 10027*

²*Center for Computational Quantum Physics, Flatiron Institute, 162 5th Avenue, New York, NY 10010*

(Dated: January 14, 2021)

We show that in excitonic insulators with s -wave electron-hole pairing, an applied electric field (either pulsed or static) can induce a p -wave component to the order parameter, and further drive it to rotate in the $s + ip$ plane, realizing a Thouless charge pump. In one dimension, each cycle of rotation pumps exactly two electrons across the sample. Higher dimensional systems can be viewed as a stack of one dimensional chains in momentum space in which each chain crossing the fermi surface contributes a channel of charge pumping. Physics beyond the adiabatic limit, including in particular dissipative effects is discussed.

Controlling many-body systems, and in particular using appropriately applied external fields to ‘steer’ order parameters of symmetry broken phases, has emerged as a central theme in current physics [1–8]. The excitonic insulator (EI) is state of matter first proposed in the 1960s [9–12] with an order parameter defined as a condensate of bound electron hole pairs that activates a hybridization between two otherwise (in the simplest case) decoupled bands and opens a gap in the electronic spectrum. Several candidate materials including electron-hole bilayers [13–15], Ta₂NiSe₅ [16–21], 1T-TiSe₂ [22–25] and monolayer WTe₂ [26] are objects of current intensive study; recent work [15, 27–32] has pointed out their possible topological aspects. While the early theories of EI considered a one component order parameter, typically of inversion symmetric s -wave type, realistic interactions also allow for electron-hole pairing in sub-dominant channels including p -wave (inversion-odd) ones. In equilibrium, the s -wave ground state is favored, with the potential for p -wave order revealed by its fluctuations accompanied by dipole moment oscillations: the ‘Bardasis-Schrieffer’ collective mode [33].

In this paper we show that applied electric fields can steer the order parameter to rotate in the space of s and p symmetry components, as shown in Fig. 1(a), leading to a realization of the ‘Thouless charge pump’ [34–37], providing quantized charge transport across an insulating sample.

The minimal model of an EI involves two electron bands shown in Fig. 1(b): a valence band with energy $\xi_{v,k}$ that disperses downwards from a high symmetry point (taken to have zero momentum) and a conduction band ($\xi_{c,k}$) that disperses upwards. For simplicity we assume that their energies are equal and opposite ($\xi_c = -\xi_v = \xi$). Relaxing this assumption does not change our results in an essential way. Defining the overlap $G = 2\xi_{v,0}$, we distinguish the ‘BCS’ case $G > 0$ where the two bands cross at a fermi wavevector k_F with fermi velocity v_F as shown by the dashed lines, leading to electron and hole pockets, and the ‘BEC’ case where $G < 0$ and the bands do not cross. Excitonic order corresponds to the spontaneous formation of a hybridization between the two bands due to the electron-electron interaction V , leading to an order parameter $\Delta(k) = \sum_{k'} V_{k-k'} \langle \psi_{c,k'}^\dagger \psi_{v,k'} \rangle + c.c.$ where $\psi_{c/v,k}$ is the electron annihilation operator at momentum k of the conduction/valence band and V_q is the Fourier transform of the density-density interaction potential $V(r)$.

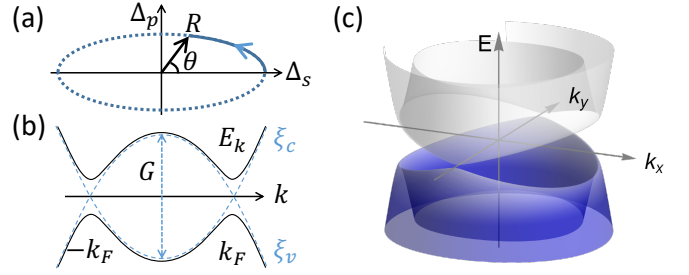


FIG. 1. (a) The $s + ip$ plane for the excitonic order parameter, with electric field-driven evolution shown as dashed line. (b) The quasiparticle dispersion in a one dimensional EI (solid lines) along with bands in metallic phase (dashed lines). (c) The band dispersion of a two dimensional EI with an $s + ip$ order parameter and $\Delta_s \ll \Delta_p$.

The s -wave order parameter $\Delta_s(k)$ is invariant under crystal symmetry operations while p -wave order parameters are odd under inversion: $\Delta_p(k) = -\Delta_p(-k)$, and often transform as a multi-dimensional representation of the crystal symmetry group. For simplicity we neglect the k -dependence of Δ_s , and define $\Delta_p(k) = \Delta_p f_k$ where the pairing function f_k carries the momentum dependence and satisfies $\max(|f_{k_F}|) = 1$. We focus on the p_x pairing channel which is induced by the x -direction electric fields we consider here. While the qualitative conclusions hold generically for all spatial dimensions, we will indicate the dimensionality if a specific d -dimensional system is discussed where the momentum k means a d -dimensional vector.

Writing the partition function Z as a path integral over fermion fields $\psi = (\psi_c, \psi_v)$, performing a Hubbard-Stratonovich transformation of the interaction term in the excitonic pairing channel and subsuming the intraband interaction into ξ one obtains the action (see [38] Sec. I)

$$S = \int d\tau dr \left\{ \psi^\dagger (\partial_\tau + H_m) \psi + \frac{1}{g_s} |\Delta_s|^2 + \frac{1}{g_p} |\Delta_p|^2 \right\} \quad (1)$$

as an integral over space-time (r, τ) and the partition function is $Z = \int D[\bar{\psi}, \psi] D[\bar{\Delta}, \Delta] e^{-S}$. For physically reasonable interactions such as the screened Coulomb interaction, the s -wave pairing interaction g_s is typically the strongest while g_p is the leading subdominant one. We may write the mean

field Hamiltonian as $\int dr \psi^\dagger H_m \psi = \sum_k \psi_k^\dagger H_m^k \psi_k$ with

$$H_m^k[\Delta_s, \Delta_p] = \xi_k \sigma_3 + \Delta_s \sigma_1 + \Delta_p f_k \sigma_2 \quad (2)$$

where σ_i are the Pauli matrices acting in the c/v band space. The vector potential A enters Eq. (2) through the minimal coupling $k \rightarrow k - A$ required by local gauge invariance (electric field is $E = -\partial_t A$) and we set electron charge e , speed of light and the Planck constant \hbar to be one. Interband dipolar couplings could also occur [6, 39] but do not affect our results. Since the global phase is not important, we choose the s -wave order parameter to be real. As we will show, the system develops an electrical polarization as a p -wave component $\pi/2$ out of phase with the equilibrium Δ_s is introduced. Due to an emergent ‘particle hole’ symmetry in the BCS weak coupling case defined as $|\Delta_s|, |\Delta_p| \ll G$ which we focus on, applied electric fields create Δ_p primarily in this channel (see Sec. VI A of [38] for a rigorous proof), so we write p -wave pairing in the σ_2 channel [33]. The quasi-particle spectrum is $E_k = \pm \sqrt{\xi_k^2 + \Delta_s^2 + \Delta_p^2 f_k^2}$. As shown by Fig. 1(c), the spectrum will have gapless points (nodes) at $(k_x, k_y) = (0, \pm k_F)$ in the pure p -wave state ($\Delta_s = 0$) in two dimensions (2D).

Charge pump—Spatially uniform changes in $\Delta_{s,p}$ produce uniform currents $J = \langle \sum_k \partial_k H_m^k \rangle$ (see [38] Sec. II), whose time integral from the initial $(\Delta_s, \Delta_p) = (\Delta, 0)$ to the final point then gives the pumped charge P (difference of polarization between the final state and the initial state). In a one dimensional (1D) system, P has a geometrical meaning [36, 40] in the limit of slow order parameter dynamics. It is the flux of the Berry curvature 2-form B through the 2D surface S spanned by the occupied 1D crystal momentum k and the time varying trajectory of $\Delta_{s,p}$, or alternatively by the line integral of the Berry connection $\mathcal{A}_\mu = i \langle \psi | \partial_\mu | \psi \rangle$ around its boundary:

$$P = \frac{1}{2\pi} \int_S dS \cdot B = \frac{1}{2\pi} \oint dl \cdot \mathcal{A} \quad (3)$$

where $\mu = (k, \Delta_s, \Delta_p)$ (see Fig. 2).

The Berry curvature B from the valence band of Eq. (2) is sourced by monopoles at the points $\xi_k = \Delta_s = \Delta_p = 0$, i.e., the points $(k, \Delta_s, \Delta_p) = (\pm k_F, 0, 0)$ each of which has monopole charge 1. If the order parameter evolution completes a full cycle on the $s + ip$ plane, S becomes the surface of the 2-torus shown in Fig. 2(a) and the net charge pumped is the total flux from the enclosed monopoles which is an integer $N = 2$, the Chern number of the process. This quantized change in the polarization is known as the Thouless pump [34], a topological phenomenon immune to disorder. Note that the monopoles exist only for the ‘BCS’ ($G > 0$, band inversion) case where the excitons strongly overlap such that charge can jump between them. In the ‘BEC’ case $\xi_k \neq 0$ for all k and there are no monopoles enclosed in S (see [38] Sec. II C).

To compute the polarization for the case the order parameter does not complete a full cycle, we use the line integral approach. For notational simplicity, we suppress the subscripts ‘ k ’ without causing ambiguities. An explicit

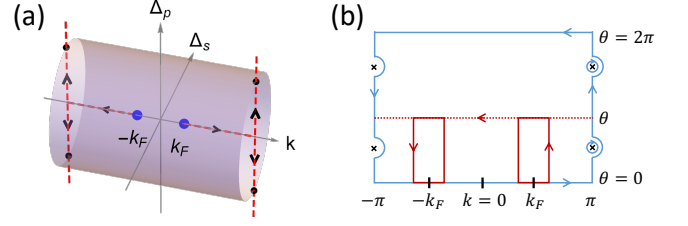


FIG. 2. (a) The surface S in the (k, Δ_s, Δ_p) space used to calculate the flux of the Berry curvature for a 1D EI for which the order parameter evolution completes a full cycle in the $s + ip$ plane. The left and right ends of the cylinder are identified so that S is a 2-torus. Blue dots are Berry curvature monopoles and red dashed lines are ‘Dirac strings’ with direction shown by black arrows. (b) The surface of the torus shown in (a) parametrized by k and θ with $k = \pm\pi$ and $\theta = 0, 2\pi$ identified. The blue contours yield the charge pumped during a full cycle. The red rectangles are used to compute the flux for a partial cycle in the BCS limit.

expression for the valence band wave function from (2) at (k, Δ_s, Δ_p) is

$$|\psi\rangle = (-v^*, u^*) = \frac{1}{\sqrt{2E(E - \xi)}} (\xi - E, \Delta^*) \quad (4)$$

where $\Delta = \Delta_s + i\Delta_p f_k \equiv |\Delta| e^{i\phi}$ and $|u|^2 (|v|^2) = \frac{1}{2} (1 \pm \frac{\xi}{E})$. The Berry connection $\mathcal{A}_\mu = |u|^2 \partial_\mu \phi$ has singularities associated with the Dirac strings, the intersections of which with S (marked by crosses in Fig. 2(b)) must be correctly treated in the evaluation of the line integral. Noting that $|u|^2 \rightarrow 0$ when $\xi \ll -|\Delta|$ and $|u|^2 \rightarrow 1$ when $\xi \gg |\Delta|$, we see that in the weak coupling BCS limit the contour can be collapsed to the red rectangles in Fig. 2(b). Parameterizing S using k and the angle θ defined by $\Delta_s + i\Delta_p = Re^{i\theta}$ in Fig. 1(a), one observes that the polarization of an state on the $s + ip$ plane depends only on the angle θ . Specifically, we found

$$P = \theta / \pi \quad (5)$$

for a 1D EI (see [38] Sec. II). This may be understood by noting that the low energy physics around $\pm k_F$ is of two massive Dirac models, each of which realizes a Goldstone-Wilczek [41] mechanism of charge pumping.

Higher dimensional systems can be viewed as 1D chains along x direction stacked in momentum space. For a 2D circular fermi surface one finds

$$P(\theta) = \begin{cases} \frac{k_F}{2\pi} \tan \frac{\theta}{2} & (0 < \theta < \pi/2) \\ \frac{k_F}{2\pi} \left(2 - \cot \frac{\theta}{2} \right) & (\pi/2 < \theta < \pi) \\ \frac{k_F}{\pi} + P(\theta - \pi) & (\pi < \theta < 2\pi) \end{cases} \quad (6)$$

A full cycle pumps exactly two electrons along each 1D momentum chain that crosses the fermi surface, giving

$$P_{1D} = 2, \quad P_{2D} = \frac{2k_F}{\pi}, \quad P_{3D} = \frac{k_F^2}{2\pi} \quad (7)$$

for 1D, 2D and three dimensional (3D) isotropic systems respectively.

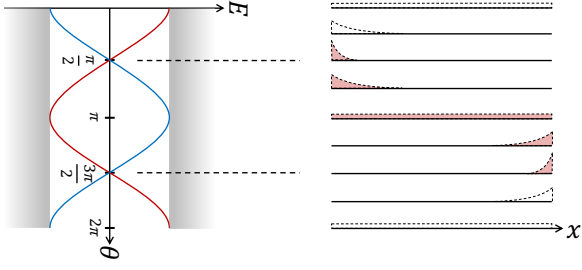


FIG. 3. Left is the evolution of the edge state energies as a function of θ . Right is the spatial profile of one of the two edge states (labeled by red line on the left) neglecting its quick oscillating detail. Being filled means the state is occupied. The blue edge state is not shown but is the mirror image of the red one.

Although the charge pump is a bulk property carried by all valence band electrons, it is also revealed by the evolution of edge states [42] as Δ_s and Δ_p are varied, as shown in Fig. 3 for a 1D wire connected with reservoirs. In the BCS limit, with open boundary conditions $\psi(0) = \psi(L) = 0$, there are two edge states

$$\psi_{\pm} = \frac{1}{C_{\pm}} (1, \pm 1) \sin(k_F x) e^{\mp x \Delta_p / v_F}, \quad E = \pm \Delta_s \quad (8)$$

where C_{\pm} is a normalization constant. We suppose $\Delta_s + i\Delta_p = R e^{i\theta}$ and follow the evolution of ψ_+ as θ is varied (see Fig. 3). At $\theta = 0$ the state is delocalized and unoccupied with energy R . As θ is increased the state becomes localized near $x = 0$ and decreases in energy. When θ passes through $\pi/2$, the state becomes maximally localized and becomes occupied by an electron from the left reservoir since its energy crosses the chemical potential. As θ further increases the state becomes delocalized and then localized at the right edge, delivering its electron to the right reservoir when θ crosses $3\pi/2$. Considering the ψ_- state during the same cycle, two electrons in total are pumped. In higher dimensions, each 1D k_x chain crossing the Fermi surface has a similar edge state evolution (see [38] Sec. III).

Dynamics—The coupled dynamics of electrons and the order parameters in the presence of an applied electric field is described by the action Eq. (1). To understand the qualitative dynamics, we use a low energy effective Ginzburg-Landau Lagrangian

$$L(\Delta_s, \Delta_p; E) = F - K + L_{\text{drive}} \quad (9)$$

for fields Δ_s, Δ_p obtained by integrating out the Fermions (see [38] Sec. IV). The dynamics is given by the standard Euler-Lagrange equation $\frac{d}{dt} \frac{\delta L}{\delta \dot{\Delta}_i} = \frac{\delta L}{\delta \Delta_i}$ and is that of a point particle moving in the landscape defined by F , with kinetic energy K and driven by an electric field through L_{drive} . We find

$$L_{\text{drive}} = -P(\theta)E - s(\Delta_s, \Delta_p)E^2 + O(E^3) \quad (10)$$

where P is the adiabatic polarization in Eqs. (5) or (6), $s = \lim_{\omega \rightarrow 0} \sigma(\omega)/(2i\omega)$ and $\sigma(\omega)$ is the optical conductivity from virtual interband excitations (see [38] Sec. IV). It is

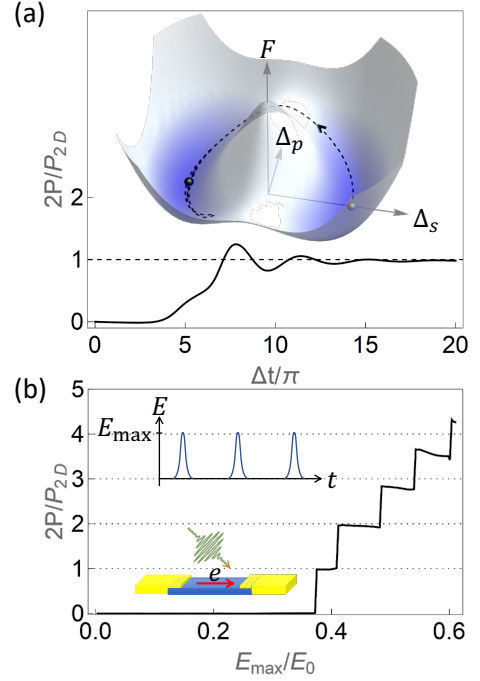


FIG. 4. Electric field pulse induced dynamics of a 2D isotropic EL. (a) The polarization as a function of time during the dynamics with P_{dis} being small. Inset is the free energy landscape $F(\Delta_s, \Delta_p)$ plotted on the $s + ip$ plane. Lower energy appears bluer. The black dashed order parameter trajectory is caused by a pulse $E(t) = E_{\text{max}} \tanh'((t - t_0)/w)$ with maximum electric field $E_{\text{max}} = 0.39E_0$. (b) The pumped charge by a single pulse as a function of E_{max} . The units are $P_{2D} = 2k_F/\pi$ and $E_0 = \Delta^2/v_F$. Top inset is a schematic of a train of well separated pulses which can induce a ‘steady’ current. Bottom inset is a schematic of the device with EI shown in blue and the contacts in gold. The parameters are $g_s v = 0.3$, $g_p v = 0.58$, $\Delta = 2\Lambda e^{-1/(g_s v)}$, $\gamma = 0.07\Delta$ and $w = 2\pi/(2\Delta)$.

natural that electric field couples linearly to the polarization and therefore provides a ‘force’ $E \partial_\theta P$ to rotate the order parameter in the Δ_s, Δ_p plane.

$F(\Delta_s, \Delta_p)$ gives the potential landscape in which the dynamics takes place; it has the anisotropic ‘Mexican hat’ form shown in Fig. 4(a). For (quasi) 1D systems in the weak coupling BCS limit [43, 44]:

$$F = -v \left(\Delta_s^2 + \Delta_p^2 \right) \ln \frac{2\Lambda}{\sqrt{\Delta_s^2 + \Delta_p^2}} + \frac{1}{g_s} \Delta_s^2 + \frac{1}{g_p} \Delta_p^2 \quad (11)$$

where v is density of states in the metallic phase and $\Lambda \gg \sqrt{\Delta_s^2 + \Delta_p^2}$ is a high energy cutoff [10]. The first term becomes $-v \int \frac{d\theta_k}{2\pi} \left(\Delta_s^2 + \Delta_p^2 \cos^2 \theta_k \right) \ln \left(2\Lambda / \sqrt{\Delta_s^2 + \Delta_p^2 \cos^2 \theta_k} \right)$ for a 2D isotropic Fermi surface and $\frac{d\theta_k}{2\pi} \rightarrow \frac{\sin \theta_k d\theta_k d\phi_k}{4\pi}$ for 3D where θ_k and ϕ_k are angular variables on the Fermi surface. The landscape has a local maximum at $R = 0$ surrounded by a trough at $R(\theta)$ of lower values of F . The ground state minima are at $(\pm \Delta, 0)$ and the pure p-wave phases at $(0, \pm \Delta_{p0})$ are saddle points with energy higher by $F_b = v(\Delta^2 - c\Delta_{p0}^2)/2$ where c is a constant depending on the

space dimension.

We may estimate the minimal electric field required to drive the system from the minimum through the p -wave saddle point by equating the potential energy barrier F_b to the work $EP(\theta = \pi/2) + \mathcal{O}(E^2)$ done by the electric field, obtaining

$$E_c \approx \kappa E_0, \quad E_0 = \Delta/\xi^0 = \Delta^2/\nu_F \quad (12)$$

where $\xi^0 = \nu_F/\Delta$ is the coherence length (exciton size), $\kappa = \frac{1}{\pi}(1 - \Delta_{p0}^2/\Delta^2)$ in 1D and $\kappa = \frac{1}{2} - \frac{1}{4}\frac{\Delta_{p0}^2}{\Delta^2}$ in 2D, and E_0 is at the order of the dielectric breakdown field. For $\nu_F = 10^6$ m/s, $\Delta = 10$ meV and $\Delta_{p0} \ll \Delta$, such as the case of electron hole bilayers, the threshold field is $E_c \sim 10^3$ V/cm which can be easily achieved by modern optical technique. For a 100 meV gap such as that in Ta_2NiSe_5 [16, 17] (assuming it is in the BCS regime), the threshold field is about 10^5 V/cm. At such large field, $\mathcal{O}(E^2)$ terms in the Lagrangian will be important, which pushes the order parameter closer to zero but does not destroy the qualitative dynamics in the transient regime (See [38] Sec. IV D).

The dynamical term K has a relatively simple form if the gap never closes on the Fermi surface and the order parameter variation timescale is long compared to the inverse of the gap. For example for (quasi) 1D

$$K \approx \nu(R^2/R^2 + 3\dot{\theta}^2)/12 \quad (13)$$

to lowest order in time derivatives. For higher dimensions with closed Fermi surfaces, there are $\mathcal{O}(1)$ changes to the coefficients and, crucially, dissipation and time non-locality arises from quasiparticle excitations near the nodes of the p -wave gap when Δ_s passes zero. This dissipation also brings a correction to the pumped charge: $P \rightarrow P_{2D} + P_{\text{dis}}$. To estimate P_{dis} , we observe that as the order parameter passes this gapless regime with a velocity $\dot{\Delta}_s$, the probability for exciting a particle-hole pair at k is given by the Landau-Zener formula [45]: $P_k = e^{-2\pi\delta_k^2/|\partial_t 2\Delta_s|}$ where $\delta_k = \sqrt{\xi_k^2 + \Delta_p^2}f_k^2$ is half of its minimal excitation energy during the dynamics. In 2D, summing over momenta, one obtains the number of excited quasi particles $N = \frac{k_F}{2\pi^2\nu_F}|\frac{\dot{\Delta}_s}{\Delta_p}|$ and the non-adiabatic correction to the pumped charge

$$P_{\text{dis}} = -P_{2D} \frac{1}{8\pi^2} \frac{|\dot{\Delta}_s|}{\Delta_p^2} \quad (14)$$

valid if $\sqrt{|\dot{\Delta}_s|} \ll |\Delta_p|$ (see [38] Sec. VI C). Therefore, if the sub-dominant p -wave coupling constant is too small such that $\Delta_{p0} \sim \Lambda e^{-\frac{1}{g_{pv}}} < \sqrt{|\dot{\Delta}_s|/(8\pi^2)}$, this dissipative correction will dominate over the adiabatic charge.

Numerics and Experiment—We numerically solved the mean field dynamics implied by Eq. (1) for a BCS weak coupling EI in 2D, driven by a train of widely separated electric

field pulses (Fig. 4(b)). Mean field dynamics [46] means that each momentum state evolves in the time dependent mean field $(\Delta_s, \Delta_p f_{k-A}, \xi_{k-A})$ with $\Delta_{s,p}$ determined self consistently by the gap equation, neglecting any spatial fluctuations. We include a weak phenomenological damping γ to represent energy loss caused by, e.g., a phonon bath (see [38] Sec. VI). Each pulse drives the order parameter along the trajectory shown as the black dashed line in Fig. 4(a), advancing it by $\theta = \pi$ to stabilize the system in the other s -wave ground state. The total duration of the evolution from one minimum to the next is $T_s \approx 20\pi/\Delta$ and the amount of charge pumped is $WP_{2D}/2$ where W is the width of the sample, as shown by Fig. 4(a). In a train of pulses with inter pulse separation $T_0 \gg T_s$, each pulse advances the order parameter from one minimum to the next and allows it to stabilize before next pulse arrives, leading to a time-averaged current $I_0 = eWk_F/(\pi T_0)$. For a $10\mu\text{m}$ wide sample with normal state carrier density of 10^{12}cm^{-2} and inter pulse time $T_0 = 1\text{ns}$, the current is $I_0 = 255\text{nA}$ considering spin degeneracy.

A minimum field strength $\sim E_c$ (12) is required: as the maximum electric field E_{max} of the pulse is increased beyond the threshold, the charge pumping (DC current) will onset sharply, as shown in Fig. 4(b). As E_{max} further increases, each pulse induces a rotation of more cycles which pumps more charge, giving rise to the step structure. Deviations from perfect quantization arise from fast order parameter dynamics caused by the short duration pulse. A precisely engineered long duration pulse can substantially reduce these deviations; see [38] Sec. V.

A static electric field in the DC transport regime could also drive such an order parameter rotation and charge pumping. However, unlike the case of well separated pulses, there is no time break to dump the generated heat into the environment which might destroy the system.

Discussion—We have shown theoretically that a Thouless charge pump may be realized as a collective many-body effect arising from order parameter steering in BCS type excitonic insulators. Similar dynamics and charge pumping can occur in general when the ground state order parameter and the sub dominant one have different parities under inversion. Its observation would provide both a verification of order parameter steering and a probe of the excitonic insulating state, in particular, distinguishing BCS and BEC states. It is interesting to study the dynamics in the vicinity of the BCS-BEC crossover and effects beyond mean field.

ACKNOWLEDGMENTS

We acknowledge support from the Energy Frontier Research Center on Programmable Quantum Materials funded by the US Department of Energy (DOE), Office of Science, Basic Energy Sciences (BES), under award No. DE-SC0019443. We thank W. Yang, D. Golez and T. Kaneko for helpful discussions.

-
- [1] A. Kirilyuk, A. V. Kimel, and T. Rasing, *Rev. Mod. Phys.* **82**, 2731 (2010).
- [2] J. H. Mentink, K. Balzer, and M. Eckstein, *Nature Communications* **6**, 6708 (2015).
- [3] T. Byrnes, N. Y. Kim, and Y. Yamamoto, *Nature Physics* **10**, 803 (2014).
- [4] J. Zhang and R. Averitt, *Annu. Rev. Mater. Res.* **44**, 19 (2014).
- [5] D. N. Basov, R. D. Averitt, and D. Hsieh, *Nature Materials* **16**, 1077 (2017).
- [6] D. Golež, P. Werner, and M. Eckstein, *Phys. Rev. B* **94**, 035121 (2016).
- [7] M. Claassen, D. M. Kennes, M. Zingl, M. A. Sentef, and A. Rubio, *Nature Physics* **15**, 766 (2019).
- [8] Z. Sun and A. J. Millis, *Phys. Rev. X* **10**, 021028 (2020).
- [9] N. F. Mott, *Philos. Mag.* **6**, 287 (1961).
- [10] A. Kozlov and L. Maksimov, *Sov. J. Exp. Theor. Phys.* **21**, 790 (1965).
- [11] D. Jérôme, T. M. Rice, and W. Kohn, *Phys. Rev.* **158**, 462 (1967).
- [12] T. Portengen, T. Östreich, and L. J. Sham, *Phys. Rev. B* **54**, 17452 (1996).
- [13] M. M. Fogler, L. V. Butov, and K. S. Novoselov, *Nat. Commun.* **5**, 4555 (2014).
- [14] J. I. A. Li, T. Taniguchi, K. Watanabe, J. Hone, and C. R. Dean, *Nature Physics* **13**, 751 (2017).
- [15] L. Du, X. Li, W. Lou, G. Sullivan, K. Chang, J. Kono, and R.-R. Du, *Nature Communications* **8**, 1971 (2017).
- [16] Y. F. Lu, H. Kono, T. I. Larkin, A. W. Rost, T. Takayama, A. V. Boris, B. Keimer, and H. Takagi, *Nat. Commun.* **8**, 1 (2017).
- [17] D. Werdehausen, T. Takayama, M. Höppner, G. Albrecht, A. W. Rost, Y. Lu, D. Manske, H. Takagi, and S. Kaiser, *Science Advances* **4**, eaap8652 (2018).
- [18] Y. Wakisaka, T. Sudayama, K. Takubo, T. Mizokawa, M. Arita, H. Namatame, M. Taniguchi, N. Katayama, M. Nohara, and H. Takagi, *Phys. Rev. Lett.* **103**, 026402 (2009).
- [19] T. Kaneko, T. Toriyama, T. Konishi, and Y. Ohta, *Phys. Rev. B* **87**, 035121 (2013).
- [20] K. Sugimoto, S. Nishimoto, T. Kaneko, and Y. Ohta, *Phys. Rev. Lett.* **120**, 247602 (2018).
- [21] G. Mazza, M. Rösner, L. Windgätter, S. Latini, H. Hübener, A. J. Millis, A. Rubio, and A. Georges, *Phys. Rev. Lett.* **124**, 197601 (2020).
- [22] A. Kogar, M. S. Rak, S. Vig, A. A. Husain, F. Flicker, Y. I. Joe, L. Venema, G. J. MacDougall, T. C. Chiang, E. Fradkin, J. Van Wezel, and P. Abbamonte, *Science* **358**, 1314 (2017).
- [23] H. Cercellier, C. Monney, F. Clerc, C. Battaglia, L. Despont, M. G. Garnier, H. Beck, P. Aebi, L. Patthey, H. Berger, and L. Forró, *Phys. Rev. Lett.* **99**, 146403 (2007).
- [24] T. Kaneko, Y. Ohta, and S. Yunoki, *Phys. Rev. B* **97**, 155131 (2018).
- [25] C. Chen, B. Singh, H. Lin, and V. M. Pereira, *Phys. Rev. Lett.* **121**, 226602 (2018).
- [26] Y. Jia, P. Wang, C.-L. Chiu, Z. Song, G. Yu, B. J., S. Lei, S. Klemen, F. A. Cevallos, M. Onyszczyk, N. Fishchenko, X. Liu, G. Farahi, F. Xie, Y. Xu, K. Watanabe, T. Taniguchi, B. A. Bernevig, R. J. Cava, L. M. Schoop, A. Yazdani, and S. Wu, “Evidence for a monolayer excitonic insulator,” (2020), [arXiv:2010.05390 \[cond-mat.mes-hall\]](https://arxiv.org/abs/2010.05390).
- [27] Y. Hu, J. W. F. Venderbos, and C. L. Kane, *Phys. Rev. Lett.* **121**, 126601 (2018).
- [28] R. Wang, O. Erten, B. Wang, and D. Y. Xing, *Nat. Commun.* **10**, 1 (2019).
- [29] L.-H. Hu, R.-X. Zhang, F.-C. Zhang, and C. Wu, *Phys. Rev. B* **102**, 235115 (2020).
- [30] D. Varsano, M. Palummo, E. Molinari, and M. Rontani, *Nature Nanotechnology* **15**, 367 (2020).
- [31] E. Perfetto and G. Stefanucci, *Phys. Rev. Lett.* **125**, 106401 (2020).
- [32] Y. Hou, R. Wang, R. Xiao, L. McClintock, H. Clark Travaglini, J. Paulus Francia, H. Fetsch, O. Erten, S. Y. Savrasov, B. Wang, A. Rossi, I. Vishik, E. Rotenberg, and D. Yu, *Nature Communications* **10**, 5723 (2019).
- [33] Z. Sun and A. J. Millis, *Phys. Rev. B* **102**, 041110(R) (2020).
- [34] D. J. Thouless, *Phys. Rev. B* **27**, 6083 (1983).
- [35] M. J. Rice and E. J. Mele, *Phys. Rev. Lett.* **49**, 1455 (1982).
- [36] R. D. King-Smith and D. Vanderbilt, *Phys. Rev. B* **47**, 1651(R) (1993).
- [37] Y. Zhang, Y. Gao, and D. Xiao, *Phys. Rev. B* **101**, 041410(R) (2020).
- [38] See Supplemental Material for details of derivation.
- [39] Y. Murakami, D. Golež, T. Kaneko, A. Koga, A. J. Millis, and P. Werner, *Phys. Rev. B* **101**, 195118 (2020).
- [40] R. Resta, *Rev. Mod. Phys.* **66**, 899 (1994).
- [41] J. Goldstone and F. Wilczek, *Phys. Rev. Lett.* **47**, 986 (1981).
- [42] W. Yang, C. Xu, and C. Wu, *Phys. Rev. Research* **2**, 042047 (2020).
- [43] A. Altland and B. D. Simons, *Condensed Matter Field Theory* (Cambridge University Press, Cambridge, 2010).
- [44] Z. Sun, M. M. Fogler, D. N. Basov, and A. J. Millis, *Phys. Rev. Research* **2**, 023413 (2020).
- [45] C. Wittig, *J. Phys. Chem. B* **109**, 8428 (2005).
- [46] R. A. Barankov, L. S. Levitov, and B. Z. Spivak, *Phys. Rev. Lett.* **93**, 160401 (2004).

Supplemental Material for ‘Topological charge pumping in excitonic insulators’

CONTENTS

Acknowledgments	4
References	5
I. The Hamiltonian	1
A. The pairing interactions	2
II. Computation of the polarization	3
A. Polarization	4
B. Berry Connection and Berry Curvature	4
C. BCS-BEC crossover	5
D. Pumped charge for arbitrary rotation angle	5
E. Current response in time domain	6
III. Edge states	7
IV. The Ginzburg-Landau action	8
A. Static free energy landscape	8
B. Kinetic energy	9
1. Dissipative terms	9
2. In time domain	10
C. The drive term	12
V. The adiabatic transport scheme	12
A. Description	12
B. Derivation	13
VI. Exact mean field dynamics	14
A. Pseudo spin representation	14
1. Proof of why the dynamics is confined within the $s + ip$ plane in the BCS weak coupling case	14
B. ‘Super-current’ in 1D systems	15
C. Dynamics of the node in 2D: Landau-Zener formula	16
1. The pumped charge around the node	17

I. THE HAMILTONIAN

We base our discussion on the two-band spinless Fermion Hamiltonian that is a minimal model for excitonic insulators:

$$H = \int dr \left[\psi^\dagger (\sigma_3 \xi_{p-A} + \phi_0) \psi \right] + \int dr dr' V(r-r') \rho(r) \rho(r') \quad (\text{S1})$$

where $\rho(r) = \psi^\dagger(r) \psi(r)$ is the local density at position r , $\psi^\dagger = (\psi_c^\dagger, \psi_v^\dagger)$ is the two component electron creation operator with c/v labeling the conduction/valence band, $\xi_p = \epsilon_p - \mu$ is the kinetic energy shifted by the chemical potential, $p = -i\hbar\nabla$, σ_i are the Pauli matrices in $c-v$ space, $(\phi_0, A) \equiv A_\mu$ is the electromagnetic (EM) potential and we have set the electron charge, the speed of light and Planck constant \hbar to be 1. In the non interacting case, the overlap of the bands gives rise to an electron and a hole pocket, each with the Fermi momentum k_F , Fermi velocity v_F , Fermi level density of states ν and carrier density $n/2$. We choose the gauge $\phi_0 = 0$ in this paper.

The interaction is assumed to be density-density type, e.g., $V(r) = 1/|r|$ for the Coulomb interaction. We denote its Fourier transform at momentum q as V_q . The repulsive interaction is effectively attractive between electrons and holes and can induce pairing in several angular momentum channels, in formal analogy to Cooper pairing in superconductors. We write the model as a fermionic path integral so the partition function is $Z = \int D[\bar{\psi}, \psi] e^{\int \bar{\psi} \partial_\tau \psi - H[\psi]}$ and decouple the interaction in

the electron hole pairing channel: $Z = \int D[\bar{\psi}, \psi] D[\bar{\Delta}, \Delta] e^{-S[\psi, \Delta]}$. Note that ‘ D ’ means functional field integral. The Hubbard-Stratonovich fields Δ then represent the order parameters. The interband interaction term in Eq. (SI) can be decomposed into symmetry channels labeled by l as $\hat{V}_{\text{inter}} = \sum_l g_l \hat{b}_l^\dagger \hat{b}_l$ where $\hat{b}_l = \sum_k f_k^l \psi_{c,k}^\dagger \psi_{v,k}$ and f_k^l are the representation functions (pairing functions) of the point symmetry group. Therefore, we can resolve Δ into pairing functions as $\Delta_k = \sum_l \Delta_l f_k^l$. We assume for notational simplicity that the excitonic effects occur near a high symmetry point so that lattice effects are unimportant and that the interaction effects may be restricted to the Fermi surface. In this case f^l become the usual d -dimensional rotational harmonics and the interaction V_q is parameterized by the momentum transfer q connecting two points on the Fermi surface. We focus on s pairing (f_k^s has the full point symmetry of the lattice; we take $f_k^s = 1$) and p_x pairing $f_k^p = k_x/k_F$. We denote the latter as f_k for notational simplicity.

The Hubbard Stratonovich transformed action is

$$S[\psi, \Delta_s, \Delta_p, A] = \int d\tau dr \left\{ \psi^\dagger (\partial_\tau + H_m) \psi + \frac{1}{g_s} |\Delta_s|^2 + \frac{1}{g_p} |\Delta_p|^2 \right\}. \quad (\text{S2})$$

Since the overall phase of the Hubbard Stratonovich field is not relevant for our considerations, we choose Δ_s to be real. As we will see in Sec. VIA, due to a ‘particle hole’ symmetry in the BCS weak coupling case, the main effect of an electric field is to induce a p -wave field that is $\pi/2$ out of phase with Δ_s . We restrict our attention to this case. The mean field Hamiltonian is thus $H_m^k = \xi_k \sigma_3 + \Delta_s \sigma_1 + \Delta_p f_k \sigma_2$ with real Δ_s, Δ_p and the EM vector potential enters as $k \rightarrow k - A$. Note that minimal coupling substitution is also applied to the p -wave decoupling term: $\Delta_p f_{k-A}$ although this term comes from the electron-electron interaction that contains no EM field. We discuss this choice here in terms of local gauge invariance.

In the full functional integral, the general gauge invariant form of the decoupling term is $e^{-i \int_{r_1}^{r_2} d\Lambda(l) \Delta(r_1, r_2) \psi_b^\dagger(r_1) \psi_c(r_2)}$, which preserves its form under the usual local gauge transformation $U_g : \psi(r) \rightarrow \psi(r) e^{i\theta(r)}$, $A_\mu \rightarrow A_\mu + \partial_\mu \theta(r)$. We write $\Delta(r_1, r_2) = |\Delta(r_1, r_2)| e^{i\varphi(r_1, r_2)}$; both the amplitude $|\Delta(r_1, r_2)|$ and the phase $\varphi(r_1, r_2)$ are dynamical variables. The dependence on ‘center of mass’ coordinate $r = (r_1 + r_2)/2$ gives the spatial variation of the order parameter while the dependence on $r_1 - r_2$ gives the internal structure of the electron hole pair (the momentum dependence of the pairing function). Writing the phase degrees of freedom as $\varphi(r_1, r_2) = \varphi_0(r) + (r_1 - r_2)\alpha(r)$ in the slow varying limit, the φ_0 is the usual order parameter phase and the combination $\alpha + A$ enters structure of pairing wave function as $f_{k-A-\alpha}$. Although $\alpha = 0$ in the initial ground state, one should in principle track the dynamics of α . In the weak coupling BCS limit, we may neglect the dynamics of α since its appearance is equivalent to a Δ_s in the σ_2 channel which vanishes as we will prove in Sec. VI. Even in the general case when the appearance of α must be considered at intermediate stages of the dynamics, the amount of charge pumping during a full cycle is still the quantized value given that the system finally returns to its initial state, as shown in general by Thouless [34].

If the two bands are formed by atomic orbitals having different parities, e.g., p and d orbitals, an interband dipolar moment D_0 adds the extra term $D_0 E \psi^\dagger \sigma_1 \psi$ to the Hamiltonian. This term also contributes to the EM response due to change of inter orbital hybridization. However, for a full cycle of order parameter dynamics, the amount of pumped charge won’t be affected if the initial and final states are the same such that they have the same inter orbital hybridization. The dynamics itself won’t be qualitatively affected if the interband dipole D_0 is not large compared to the dipole formed between s and p -symmetry electron and hole bound states that produce the order parameters. This is true in the BCS case since the former is proportional to the size of atomic orbitals while the latter is the size ξ^0 of the extended electron hole bound state.

A. The pairing interactions

For isotropic systems in d dimensions, the pairing interaction in channel l is

$$g_l = \frac{1}{2|f^l|^2} \int d\Omega_1 d\Omega_2 f_{k(\Omega_1)}^{l*} V_{k(\Omega_1) - k(\Omega_2)} f_{k(\Omega_2)}^l \quad (\text{S3})$$

where Ω is the angular variable on the $d-1$ dimensional Fermi surface, $k(\Omega)$ is the electron momentum at angle Ω and $|f^l|^2 = \int d\Omega |f_{k(\Omega)}^l|^2$ is the normalization factor. Since the symmetry group is $O(d)$, the d -dimensional rotations and inversions, the pairing functions f^l are d -dimensional spherical harmonics. Below we discuss 1D and 2D separately.

One dimension—There are only two pairing functions: the inversion symmetric one $f_{k_F}^s = 1, f_{-k_F}^s = 1$ and the antisymmetric one $f_{k_F}^p = 1, f_{-k_F}^p = -1$. Thus Eq. (S3) leads to $g_s = V_{q=0} + V_{q=2k_F}$ and $g_p = V_{q=0} - V_{q=2k_F}$. Since the Coulomb interaction in 1D is $V_q \sim \ln(aq)$ where a is a short distance cutoff, $V_{q=0}$ diverges Logarithmically which results in $g_s = g_p$. If the 1D system is put parallel to a metallic gate at a distance h , the screening kills the divergence of $V_{q=0}$ and renders $g_p/g_s < 1$. As h decreases, the screening get stronger and g_p/g_s decreases continuously until reaching zero at $h \ll 1/k_F$. Therefore, g_p/g_s is experimentally tunable by h .

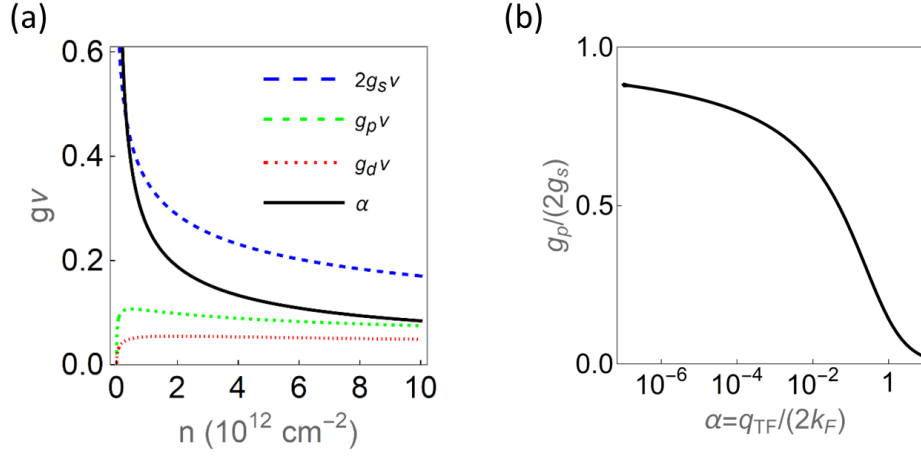


FIG. S1. Pairing interaction plots reproduced from Ref. [33]. (a) The s, p, d -wave components of the screened Coulomb interaction in 2D and the ‘fine structure constant’ $\alpha = e^2/(\epsilon\hbar v_F) = q_{\text{TF}}/(2k_F)$ as functions of electron density $n/2 = m^2 v_F^2/(4\pi\hbar^2)$ computed from Eqs. (S4) and (S5) using $m = 0.05m_e$ and $\epsilon = 10$ where m is the electron mass in the model and m_e is the vacuum electron mass. (b) The ratio $g_p/(2g_s)$ as a function of $\alpha = q_{\text{TF}}/(2k_F)$. For $\alpha \ll 1$, i.e., in the high density case, $g_p/(2g_s)$ becomes considerable and approaches one in the high density limit. Spin degeneracy is neglected.

Two dimensions—Examples are electron hole bilayers and other 2D excitonic insulators such as monolayer WTe₂ [26]. The natural pairing functions are $f_k^l = e^{il\theta_k}$ which plugged into Eq. (S3) renders $g_l = \frac{1}{2\pi} \int d\theta_k \cos(l\theta_k) V_{2k_F \sin(\theta_k/2)}$. Note that for $l = 0$, the $1/2\pi$ factor should be changed to $1/4\pi$. Since $e^{il\theta_k}$ and $e^{-il\theta_k}$ have the same g_l , we will use the real pairing functions $f_k^l = \cos(l\theta_k), \sin(l\theta_k)$ for convenience. For Thomas-Fermi screened interaction $V_q = \frac{2\pi}{\epsilon(q+q_{\text{TF}})}$ in 2D where $q_{\text{TF}}/(2k_F) = e^2/(\epsilon\hbar v_F) \equiv \alpha$ is the ‘fine structure constant’ in this system and ϵ is the dielectric constant of the environment, the s -wave pairing strength is

$$vg_s = v \frac{1}{4\pi} \int d\theta_k \frac{2\pi}{2k_F |\sin(\theta_k/2)| + q_{\text{TF}}} = \frac{\alpha}{\sqrt{1-\alpha^2}} \frac{1}{\pi} \text{Tanh}^{-1}(\sqrt{1-\alpha^2}) \quad (\text{S4})$$

and the p -wave one is

$$\begin{aligned} vg_p &= v \frac{1}{2\pi} \int d\theta_k \frac{2\pi \cos\theta_k}{2k_F |\sin(\theta_k/2)| + q_{\text{TF}}} \\ &= \alpha \left[-\frac{4}{\pi} + 2\alpha + \frac{4}{\pi} \frac{(1-2\alpha^2)}{\sqrt{1-\alpha^2}} \left(\text{Tanh}^{-1}(\sqrt{1-\alpha^2}) - \text{Tanh}^{-1}\left(\frac{\sqrt{1-\alpha^2}}{1+\alpha}\right) \right) \right]. \end{aligned} \quad (\text{S5})$$

These equations were previously given [33] and are reproduced here for convenience.

The pairing interactions are shown in Fig. S1 for the screened Coulomb interaction in 2D (reproduced from the supplemental material of Ref. [33]). To obtain a substantial $g_p/(2g_s)$, one needs the high density case where the fermi velocity is large so that the Thomas fermi wave vector is smaller than the fermi momentum: $q_{\text{TF}}/(2k_F) = \alpha = e^2/(\epsilon\hbar v_F) \ll 1$. Stronger dielectric screening of the environment can further reduce α and increase $g_p/(2g_s)$. Moreover, a non-negligible interlayer distance a changes the bare electron-hole Coulomb attraction into $V(r) = 1/\sqrt{r^2 + a^2}$, making it more nonlocal and thus can lead to a larger $g_p/(2g_s)$. Other types of interactions such as nearest neighbor Hubbard interaction (although originating from Coulomb) could give a very strong g_p , given that the band overlapping is suitable.

II. COMPUTATION OF THE POLARIZATION

In this section, we explicitly derive the charge pumping in an 1D excitonic insulator by computing the polarization P (charge pumped) as a time integral of the current J induced by adiabatic changes to the order parameter over a time interval from 0 to t and comparing the result to the formula in terms of Berry curvature, consistent with previous results [36].

A. Polarization

For convenience we reproduce the mean field Hamiltonian H_m^k and current operator J here:

$$H_m^k = \xi_k \sigma_3 + \Delta_s \sigma_1 + \Delta_p f_k \sigma_2, \quad \hat{j}_k = \psi_k^\dagger j_k \psi_k = \psi_k^\dagger (\partial_k H_m^k) \psi_k = \psi_k^\dagger (\nu_k \sigma_3 + \Delta_p \partial_k f_k \sigma_2) \psi_k, \quad J = \sum_k \hat{j}_k \quad (S6)$$

where $\nu_k = \partial_k \xi_k$ is the velocity and the energy eigenvalues are $E_k = \pm \sqrt{\xi_k^2 + \Delta_s^2 + \Delta_p^2 f_k^2}$. The current δJ in response to a change in order parameter $\delta \Delta_k = \delta \Delta_s(t) \sigma_1 + \delta \Delta_p(t) f_k \sigma_2$ is

$$\delta J(\Omega_n) = -T \sum_n \sum_k \text{Tr} \left[\frac{j_k (i\omega_n + i\Omega_n - H_m^k) \delta \Delta_k (i\omega - H_m^k)}{((\omega_n + \Omega_n)^2 + E_k^2)(\omega_n^2 + E_k^2)} \right] \quad (S7)$$

in frequency representation where $\omega_n = (2n+1)\pi T$, $\Omega_n = 2n\pi T$ are the Fermion and Boson Matsubara frequencies with $n \in \mathbb{Z}$ (not to be confused with the carrier density), T is the temperature and we have set the Boltzmann constant to be 1. Carrying out the trace over band indices, performing the frequency summation at $T = 0$ and analytically continuing $i\Omega_n$ to ω , one obtains

$$\delta J(\omega) = \frac{i\omega}{2} \left(\sum_k \frac{\nu_k f_k - \xi_k \partial_k f_k}{E_k (-\frac{\omega^2}{4} + E_k^2)} \Delta_p \delta \Delta_s(\omega) - \sum_k \frac{\nu_k f_k}{E_k (-\frac{\omega^2}{4} + E_k^2)} \Delta_s \delta \Delta_p(\omega) \right) \quad (S8)$$

Note that if the argument is ω in $\Delta_{s,p}(\omega)$, the latter means $\Delta_{s,p}(t)$ Fourier transformed into frequency representation. In the adiabatic limit we may neglect the ω^2 in the denominators; then transforming to the time domain we obtain

$$J(t) = -\frac{1}{2} \left(\sum_k \frac{\nu_k f_k - \xi_k \partial_k f_k}{E_k^3} \Delta_p \frac{\partial \Delta_s}{\partial t} - \sum_k \frac{\nu_k f_k}{E_k^3} \Delta_s \frac{\partial \Delta_p}{\partial t} \right) \quad (S9)$$

where ' J ' now means the expectation value of the current operator. Integrating in time gives the change in polarization:

$$P = \int \left(-\frac{\Delta_p (\nu_k f_k - \xi_k \partial_k f_k)}{2E_k^3} \frac{d\Delta_s dk}{2\pi} + \frac{\Delta_s \nu_k f_k}{2E_k^3} \frac{d\Delta_p dk}{2\pi} \right). \quad (S10)$$

B. Berry Connection and Berry Curvature

The Berry connection \mathcal{A}_μ is given in terms of the change in wave function under infinitesimal variation of the parameters $\mu = (k, \Delta_s, \Delta_p)$ as $\mathcal{A}_\mu = i \langle \psi | \partial_\mu | \psi \rangle$. We suppress the momentum subscripts whenever possible without causing ambiguity. Defining $\Delta = \Delta_s + i\Delta_p f_k \equiv |\Delta| e^{i\phi}$ we may write the valence band wave function as

$$|\psi\rangle = (-v^*, u^*) = \frac{1}{\sqrt{2E(E-\xi)}} (\xi - E, \Delta^*) \quad (S11)$$

implying $\mathcal{A}_\mu = |u|^2 \partial_\mu \phi$ where $|u|^2 = \frac{1}{2} \left(1 + \frac{\xi}{E} \right)$. Explicitly,

$$(\mathcal{A}_k, \mathcal{A}_{\Delta_s}, \mathcal{A}_{\Delta_p}) = \frac{|u|^2}{\Delta_s^2 + f_k^2 \Delta_p^2} (\Delta_s \Delta_p \partial_k f_k, -f_k \Delta_p, f_k \Delta_s). \quad (S12)$$

Note that \mathcal{A} has singularities ("Dirac strings") along the line $\Delta_s = \Delta_p = 0$ and also along the lines $\Delta_s = f_k = 0$ unless $|u|^2$ vanishes on parts of these lines. These are shown as dashed lines in Fig. S2(a) for the BEC case ($G < 0$). The Berry curvature $B = d\mathcal{A}$ is then

$$(B_k, B_{\Delta_s}, B_{\Delta_p}) = -\frac{1}{2E_k^3} (\xi_k f_k, \Delta_s \nu_k f_k, \Delta_p (\nu_k f_k - \xi_k \partial_k f_k)). \quad (S13)$$

Considering now the flux of B through a surface element of an oriented 2D manifold in (k, Δ_s, Δ_p) space defined by a function $s(\Delta_s, \Delta_p) = \text{constant}$ and choosing the orientation to be pointing 'inside' the cylinder in Fig. S2(a) we see by comparison to Eq. (S10) that the flux through the surface is just the polarization P . This conclusion is independent of the choice of coordinate.

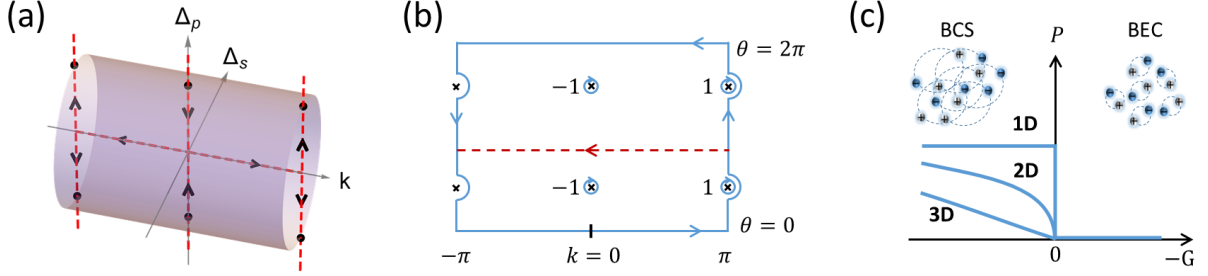


FIG. S2. (a) The (k, θ) surface S embedded in the (k, Δ_s, Δ_p) space. Shown is the BEC case where the effective G is negative in the mean field equation (band gap $-G$ is positive). In the Berry connection convention Eq. (S12), there are ‘Dirac strings’ as shown by the red dashed lines, whose intersection with S lead to the singular vortices in (b). The black arrows indicate the directions of the Dirac strings. (b) The torus parametrized with (k, θ) . The integral of the Berry curvature over the torus is converted into the loop integral on its boundary and around the singular vortices. The vortices at $k=0$ contribute opposite values to those at $k=\pi/a$, rendering the net result to be $P=0$. (c) Schematic of the pumped charge in BCS and BEC regimes of excitonic insulators.

C. BCS-BEC crossover

If the numbers of electrons and holes are separately conserved, the total number $n = \langle n_{\text{electron}} + n_{\text{hole}} \rangle = -\langle \sigma_3 \rangle + n_0$ is also conserved where n_0 is the particle number of a completely occupied band. n is the analogy to the total charge in a superconductor, and gives the constraint that shifts G from positive to negative as interaction becomes stronger such that the system crossovers from a BCS to a BEC type condensate. This is the situation in electron hole bilayers with no interlayer tunneling. Moreover, n can also be approximately fixed by gate voltage. For natural crystals, n is not fixed since there are always interband conversion mechanisms breaking this $U(1)$ symmetry. Hartree terms due to Coulomb repulsion between a/b orbitals will shift down G and induce such a crossover in this case.

In the BEC case ($G < 0$, no band inversion), there are no monopoles and the Dirac string structure looks like that in Fig. S2, rendering zero pumped charge. Intuitively, the excitons in the BEC state are tightly bound electron hole pairs that don’t overlap with other, and can be viewed as charge neutral point particles. Thus no charge transport can occur.

Therefore, there is a topological transition at $G=0$ during the BCS-BEC crossover, and the charge pumping P can be viewed as an ‘order parameter’ that separate these two regimes, as shown in Fig. S2(c). However, we have focused on the dynamics in the BCS limit in this paper while it is interesting to investigate similar dynamics in the crossover regime.

D. Pumped charge for arbitrary rotation angle

In this section we provide the details leading to Eqs. (5) and (6) of the main text. Parameterizing S using k and the angle $\theta \equiv \arg(\Delta_s, \Delta_p)$ defined in Fig. 1(a) of the main text, the Berry connection and curvature can be projected onto the (k, θ) space. In other words, The wave function can now be viewed as a function of (k, θ) and $\Delta(k, \theta) = \Delta_s + i\Delta_p f_k = |\Delta(k, \theta)|e^{i\phi(k, \theta)}$ is the pairing field at (k, θ) . Note that f_k reverses sign for positive and negative k , and that $|u|^2 = \frac{1}{2} \left(1 + \frac{\xi}{E} \right)$ is nearly zero deep inside the fermi sea ($\xi \ll -|\Delta|$) and $|u|^2 \rightarrow 1$ outside when $\xi \gg |\Delta|$.

The flux can be converted to the line integral of the Berry connection over the edge of S in Fig. 2(b) of the main text. The singularities (marked by crosses in Fig. 2(b)) are from the intersections with the Dirac strings, and must be correctly treated in the evaluation of the line integral, although they do not contain fluxes in B . For a full cycle, the edge is the blue contour together with the two small circles surrounding the two vortices. The former gives zero net contribution due to periodicity in k and θ while the latter contributes $N=2$, recovering the number of monopoles.

The polarization at arbitrary angle θ can be evaluated analytically in the BCS limit in which $|\Delta_s|, |\Delta_p| \ll G$ where a is the lattice constant. The Berry curvature is concentrated in the region $|\xi_k| \lesssim |\Delta|$ so we may perform the integral in Eq. (3) of the main text only on the red rectangles centered on $k = \pm k_F$ in Fig. 2(b) of the main text, chosen such that $u \approx 0$ on the vertical edges inside the fermi momentum $\pm k_F$ and thus $\mathcal{A}_\theta = 0$ from Eq. (S12), while $|u| \approx 1$ on the vertical edges outside the fermi momentum and $\mathcal{A}_\theta = \pm 1$. The top and bottom edges all contribute zero since $\partial_k f_k$ and thus \mathcal{A}_k are negligible around $k = \pm k_F$. Therefore, the contour integral gives

$$P = \theta / \pi \quad (\text{S14})$$

for an 1D excitonic insulator. This result may also be understood by noting that the low energy physics around $\pm k_F$ is of two massive Dirac models, each of which realizes a Goldstone-Wilczek [41] mechanism of charge pumping.

In a 2D system one has two momenta, which we choose to be parallel (k_x) and vertical (k_y) to the direction defined by the antisymmetry of f_k . The net charge pumped is then an integral over k_y of the previously obtained formula. The only change is that now $\xi_{k_x} \rightarrow \xi_{k_x, k_y}$ and it may be that for some values of k_y the sign of ξ does not change as a function of k_x , meaning that for these k_y the monopoles lie outside the torus of integration so no charge pumping occurs. In the weak coupling limit the issue may be discussed in terms of the Fermi surface of the metallic ($\Delta = 0$) phase. If the fermi surface (fermi crossings for each k_y as k_x is varied) is open the density of transferred charge is $2/a_y$ during a full cycle where a_y is the lattice constant in y direction; if the fermi surface is closed, then only the range of k_y where crossings occur gives rise to a charge pumping; thus the net density of pumped charge during a full cycle is $2k_{Fy}/\pi$ where k_{Fy} is the maximum extent of the fermi surface in the y direction.

In an isotropic 2D system, for an incomplete cycle with arbitrary θ , note that each 1D momentum chain crossing the fermi surface at $(\pm\sqrt{k_F^2 - k_y^2}, k_y) = k_F(\pm\cos\theta_k, \sin\theta_k)$ contributes a charge pumping channel described by Eq. (S14), with effective rotation angle $\varphi_{k_y} = \tan^{-1}(\cos\theta_k \tan\theta)$. Summing over all the chains, one obtains

$$P = \frac{1}{2\pi} \int_{-k_F}^{k_F} dk_y \frac{\varphi_{k_y}}{\pi} = \frac{k_F}{2\pi^2} \int_{-1}^1 dt \tan^{-1}(\sqrt{1-t^2} \tan\theta) = \frac{k_F}{2\pi} \tan \frac{\theta}{2} \quad (\text{S15})$$

for $0 < \theta < \pi/2$. Extending the above integral to higher θ , one obtains Eq. (6) of the main text.

E. Current response in time domain

In this section, we try to expand Eq. (S7) to higher orders in frequency and show that this won't give corrections to the adiabatic result. We focus on the nodes at $k = (0, \pm k_F)$ in 2D when the system is close to pure p_x -wave order. In 3D, the nodes become a nodal line and the result stays the same up to some $O(1)$ constants. Close to $(0, \Delta_p)$, the trajectory of motion is nearly along the Δ_s direction due to the saddle point structure on the free energy landscape in Fig. 4(a) of the main text. Thus it is enough to consider the current response to $\hat{\Delta}_s \equiv \partial_t \Delta_s$ in Eq. (S8): $J(\omega) = \chi_{j_x, \Delta_s}(\omega) \Delta_s(\omega)$. We assume the order parameter passes the point $(0, \Delta_p)$ with nearly constant velocity $\hat{\Delta}_s$. In the BCS limit, the second term vanishes due to the ξ factor and what remains is

$$\chi_{j_x, \Delta_s}(\omega, 0) = \sum_k v_k f_k \frac{\Delta_p}{E_k} \frac{-2i\omega}{\omega^2 - 4E_k^2} = C_0(\Delta_p, \Delta_s)(-i\omega) + C_1(\Delta_p, \Delta_s)(-i\omega)^2 + O(\omega^3) \quad (\text{S16})$$

where

$$C_0 = -\frac{1}{2} \Delta_p \sum_k v_k f_k \frac{1}{E_k^3} = -\Delta_p v \int d\theta_k \frac{1}{2\pi} v_F \cos^2 \theta_k \frac{1}{\Delta_p^2 \cos^2 \theta_k} = -v v_F \frac{1}{\Delta_p} = -\frac{1}{2\pi} \frac{k_F}{\Delta_p} \quad (\text{S17})$$

is the adiabatic current leading to Eq. (S15) and C_1 is a dissipative term that arises from quasiparticles excitations. At exactly $(0, \Delta_p)$, it is

$$C_1 = \frac{1}{-i\omega} \text{Im} \left[\sum_k \frac{v_k f_k \Delta_p}{E_k^2} \frac{2E_k}{\omega^2 - 4E_k^2} \right] = \frac{\pi}{\omega} \Delta_p \sum_k \frac{v_k f_k}{E_k^2} (\delta(\omega - 2E_k) - \delta(\omega + 2E_k)) \approx \frac{1}{8} \frac{k_F}{\Delta_p^2}. \quad (\text{S18})$$

Another source for dissipative current is the quasiparticle contributed optical conductivity from the node:

$$\sigma_{xx} = \frac{i}{\omega} \chi_{\Delta_p \partial_{k_x} f_k \sigma_2, \Delta_p \partial_{k_x} f_k \sigma_2} = \frac{i}{\omega} \frac{\Delta_p^2}{k_F^2} \chi_{\sigma_2 \sigma_2} = \frac{i}{\omega} \frac{\Delta_p^2}{k_F^2} \sum_k \frac{4E_k}{\omega^2 - 4E_k^2} \frac{\xi_k^2}{E_k^2} = \frac{1}{8} \frac{\Delta_p}{k_F v_F} + i \text{Im}[\sigma_{xx}]. \quad (\text{S19})$$

Its real part is suppressed by the small number $\Delta_p/\varepsilon_F = \Delta_p/(k_F v_F)$ and can thus be neglected.

It appears from Eq. (S18) that there is a correction to the pumped charge as $\delta P = \int dt C_1 \partial_t^2 \Delta_s$. However, if one includes higher order terms in frequency, the current response from Eq. (S16) can be written in time domain:

$$J(t) = \int_{-\infty}^t dt' \chi(t, t') \partial_{t'} \Delta_s \quad (\text{S20})$$

where

$$\begin{aligned}
\chi(t+t', t') &= \sum_k v_{x,k} f_k \frac{\Delta_p}{E_k^2} \sin(2E_k t) = v \frac{1}{2\pi} \int d\xi d\theta_k \Delta_p v_F \cos^2 \theta_k \frac{\sin(2Et)}{\xi^2 + \Delta_p^2 \cos^2 \theta_k + \Delta_s^2} \\
&= \text{node contribution} + \text{high energy state contribution} \\
&\approx v \frac{2}{2\pi} \Delta_p^{-2} v_F \int_{-\Delta_p}^{\Delta_p} d\xi dx x^2 \frac{\sin(2Et)}{\xi^2 + x^2 + \Delta_s^2} + v \frac{2\pi}{2\pi} \Delta_p v_F \int_{\Delta_p}^{\infty} d\xi \frac{\sin(2Et)}{\xi^2 + \Delta^2} \\
&\approx v \Delta_p^{-2} v_F \int_0^{\Delta_p} du u^3 \frac{\sin(2Et)}{u^2 + \Delta_s^2} + \text{high energy state contribution} \\
&\approx v \Delta_p^{-2} v_F \int_{\Delta_s}^{\Delta_p} dE (E - \Delta_s^2/E) \sin(2Et) \\
&= -\frac{1}{4} v v_F \Delta_p^{-2} \left(\partial_t + 4\Delta_s^2 \int dt \right) \frac{1}{t} (\sin(2\Delta_p t) - \sin(2\Delta_s t))
\end{aligned} \tag{S21}$$

is the response kernel which is time dependent due to the fact that Δ_s, Δ_p changes with time. Note that $E = \sqrt{\xi_k^2 + \Delta_s^2 + \Delta_p^2 f_k^2}$ in the above integrals although we neglected its subscripts for notational simplicity. If one uses the values of Δ_s, Δ_p at t' and evaluate the polarization at $t \rightarrow \infty$ by $\int dt J(t)$, one recovers exactly the adiabatic current and the topological charge pumping. Therefore, the non-adiabatic correction is beyond the scope of Eq. (S21), but lies in the fact that the state at t' is not the ground state of the instantaneous mean field Hamiltonian assumed here. We will show that this physics can be addressed in terms of exact dynamics of pseudo-spins.

III. EDGE STATES

In this section we analyse the behavior of edge states. For simplicity we focus on the weak coupling BCS limit of Eq. (S2) with open boundary condition. Linearizing the Hamiltonian near the two fermi points $\pm k_F$, we find that an edge state wave function may be written

$$\psi(x) = \phi_1 e^{-ik_F x + k_0 x} + \phi_2 e^{ik_F x + k_0 x} \tag{S22}$$

with energy $E^2 = \Delta^2 - v_F^2 k_0^2$ where $\Delta^2 = \Delta_s^2 + \Delta_p^2 f_{k_F}^2 = \Delta_s^2 + \Delta_p^2$ and we have made use of our convention $f_{k_F} = 1$. The spinor part of the wave function is

$$\phi_1 = (\Delta_s + i\Delta_p, -i v_F k_0 + E), \quad \phi_2 = (\Delta_s - i\Delta_p, i v_F k_0 + E). \tag{S23}$$

To satisfy the open boundary condition $\psi(0) = 0$, one requires $\phi_1 + \phi_2 = 0$ which yields

$$\frac{\Delta_s + i\Delta_p}{\Delta_s - i\Delta_p} = \frac{E - i v_F k_0}{E + i v_F k_0}. \tag{S24}$$

This and the relation $E^2 = \Delta^2 - v_F^2 k_0^2$ is satisfied by two solutions: $(k_0, E_+) = (-\Delta_p / v_F, \Delta_s)$ and $(k_0, E_-) = (\Delta_p / v_F, -\Delta_s)$. The corresponding wave functions are

$$\psi_{\pm} = \frac{1}{C_{\pm}} (1, \pm 1) \sin(k_F x) e^{\mp x \Delta_p / v_F}. \tag{S25}$$

Note that the subscript \pm tracks each wave function smoothly as θ varies, but does not specify either the energy or the side where the state is localized at. They are determined by the signs of their energies and the exponential factors.

The relation between the two edge states follows from symmetries. One may define two unitary operations, the ‘phase rotated inversion’ $\hat{P}_1 : (\psi_a(x), \psi_b(x)) \rightarrow (\psi_a(-x), -\psi_b(-x))$ and the $\hat{P}_2 : (\psi_a(x), \psi_b(x)) \rightarrow (\psi_b(-x), -\psi_a(-x))$. Both operators inter converts the two edge states. \hat{P}_1 is a symmetry of the mean field Hamiltonian H if the system is in a pure p -wave state while \hat{P}_2 always anti commutes with H . Therefore, ψ_{\pm} have opposite energies and will be at zero energy in a pure p -wave state.

Note that in open 1D wires connecting two reservoirs in Fig. 3 of the main text, although the edge states seem to be responsible for the charge pumping, the actual carries are all electrons in the valence band moved by continuous deformation of their wave functions, which is a bulk property. Indeed, in macroscopically long wires, the expansion and shrinking of edges states happen only in a tiny vicinity of $\theta = 0, \pi$, while the charge pumping is a continuous process as θ varies. For example in the $\theta = 0_+$ state, although there is an occupied edge state localized on the right, the other electrons in the valence band form a density distribution that has a ‘hole’ on the right, such that the total polarization is still nearly zero. In the $\theta \rightarrow \pi/2$ state, the background density distribution has a ‘half’ hole on each edge. Together with the occupied edge state on the right, it look like there is a half charge on the right edge and a half hole on the left, so that the polarization $P = 1/2$.

IV. THE GINZBURG-LANDAU ACTION

In this section we present the derivation of the semiclassical action used in the main text. The Ginzburg-Landau action for order parameter fields and the EM field is obtained by integrating out the fermions ($e^{-S[\Delta_s, \Delta_p, A]} \equiv \int D[\bar{\psi}, \psi] e^{-S[\psi, \Delta_s, \Delta_p, A]}$) in Eq. (S2), resulting in

$$S[\Delta_s, \Delta_p, A] = \text{Tr} \ln [\partial_\tau + \xi_k \sigma_3 + \Delta_s \sigma_1 + \Delta_p f_k \sigma_2] + \int dr d\tau \left(\frac{\Delta_s^2}{g_s} + \frac{\Delta_p^2}{g_p} \right) \equiv \int dr d\tau L(\Delta_s, \Delta_p, A). \quad (\text{S26})$$

The $\text{Tr} \ln$ means trace of logarithm of the infinite dimensional matrix where k should be interpreted as the spatial derivative $-i\nabla$ acting on the fermion fields, i.e., the matrix is just the kernel $\partial_\tau + H_m$ for all Fermion fields at all (r, t) in Eq. (S2) (See Sec. 6.4 of Ref. [43]). Performed in Fourier basis, it involves a summation over momenta k , the fermion Matsubara frequencies $\omega_n = (2n+1)\pi T$ ($n \in \mathbb{Z}$, T is the temperature and we have set the Boltzmann constant to be 1) and a trace of logarithm of the 2×2 matrices. Note that we have removed the absolute value symbol from Eq. (S2) since Δ_s, Δ_p are real numbers. We interpret the action as the Lagrangian for the order parameter fields moving in the presence of electric field $E = -\partial_t A$. Changing the argument A to E , we write the Lagrangian

$$L(\Delta_s, \Delta_p; E) = F - K + L_{\text{drive}} \quad (\text{S27})$$

as the sum of three terms: the static free energy landscape F , the ‘Kinetic energy’ K and drive terms. We consider each in turn.

A. Static free energy landscape

By integrating out the fermions for static Hubbard-Stratonovich fields in Eq. (S26) we obtain the free energy density (see Ref. [44] or Sec. 6.4, page 276 of Ref. [43]):

$$\begin{aligned} F &= T \int \frac{dk^d}{(2\pi)^d} \left(\sum_{\omega_n} \text{Tr} \ln [i\omega_n + \xi_k \sigma_3 + \Delta_s \sigma_1 + \Delta_p f_k \sigma_2] + \xi_k \right) + \frac{\Delta_s^2}{g_s} + \frac{\Delta_p^2}{g_p} \\ &= T \int \frac{dk^d}{(2\pi)^d} \left(\sum_{\omega_n} \ln (i\omega_n^2 - E_k^2) + \xi_k \right) + \frac{\Delta_s^2}{g_s} + \frac{\Delta_p^2}{g_p} \\ &\xrightarrow{T \rightarrow 0} - \int \frac{dk^d}{(2\pi)^d} (E_k - \xi_k) + \frac{\Delta_s^2}{g_s} + \frac{\Delta_p^2}{g_p} \end{aligned} \quad (\text{S28})$$

where $\text{Tr} \ln$ now means the trace of logarithm of the 2×2 matrix at momentum k . Note that the momentum integral has an ultraviolet (UV) cutoff Λ which is at the order of fermi energy but also affected by the Thomas-Fermi screening length [10]. Converting the integral variable to an energy ξ , we find for (quasi) 1D systems in the BCS limit:

$$F = -2\nu \int_0^\Lambda d\xi \left(\sqrt{\xi^2 + \Delta_s^2 + \Delta_p^2} - \xi \right) + \frac{1}{g_s} \Delta_s^2 + \frac{1}{g_p} \Delta_p^2 \xrightarrow{\sqrt{\Delta_s^2 + \Delta_p^2} \ll \Lambda} -\nu (\Delta_s^2 + \Delta_p^2) \ln \frac{2\Lambda}{\sqrt{\Delta_s^2 + \Delta_p^2}} + \frac{1}{g_s} \Delta_s^2 + \frac{1}{g_p} \Delta_p^2. \quad (\text{S29})$$

For a 2D isotropic Fermi surface, the first term is replaced by

$$-\nu \int \frac{d\theta_k}{2\pi} (\Delta_s^2 + \Delta_p^2 \cos^2 \theta_k) \ln \frac{2\Lambda}{\sqrt{\Delta_s^2 + \Delta_p^2 \cos^2 \theta_k}} \quad (\text{S30})$$

where θ_k runs from 0 to 2π . In 3D, one just needs to make the replacement $\frac{d\theta_k}{2\pi} \rightarrow \frac{\sin \theta_k d\theta_k d\phi_k}{4\pi}$ where θ_k is the polar angle ranging from 0 to π and ϕ_k is the azimuthal angle ranging from 0 to 2π . In 2D, as long as $g_p < 2g_s$ [33], the s -wave phase at $\Delta = 2\Lambda e^{-\frac{1}{g_s \nu} - \frac{1}{2}}$ is the ground state with energy $-\nu \Delta^2/2$ while the p -wave phase at $\Delta_{p0} = 4\Lambda e^{-\frac{2}{g_p \nu} - 1}$ is a saddle point that has energy $-\nu \Delta_{p0}^2/4$. For $g_p > 2g_s$, the ground state minimum shifts to an $s + ip$ one. Note that in d dimensions, the density of states is $\nu = \frac{\Omega_d}{(2\pi)^d} k_F^{d-1} / v_F$ where Ω_d is the surface area of the d dimensional sphere with radius 1. For example, in 2D, $\Omega_d = 2\pi$ and $\nu = \frac{1}{2\pi} k_F / v_F$.

B. Kinetic energy

The action for order parameter fluctuations is obtained by expanding Eq. (S26) as

$$S = F(\Delta_s, \Delta_p) + S_2(\delta\Delta_s, \delta\Delta_p) \quad (\text{S31})$$

around the mean field configuration to second order in $\delta\Delta_s$, $\delta\Delta_p$, temporarily neglecting the EM field. We assume spatially uniform, time-dependent order fluctuations $\hat{\Delta}_k(i\Omega_n) = (\Delta_s + \delta\Delta_s(i\Omega_n))\sigma_1 + (\Delta_p + \delta\Delta_p(i\Omega_n))f_k\sigma_2 = \Delta_s\sigma_1 + \Delta_p f_k\sigma_2 + \delta\hat{\Delta}_k(i\Omega_n)$ and find the fluctuation term

$$S_2 = -\frac{1}{2}T \sum_{\omega_n} \sum_k \text{Tr} \left[\frac{\delta\hat{\Delta}_k(i\omega_n + i\Omega_n - H_m^k) \delta\hat{\Delta}_k(i\omega - H_m^k)}{(\omega_n + \Omega_n)^2 + E_k^2} (\omega_n^2 + E_k^2)} \right] + \frac{(\delta\Delta_s)^2}{g_s} + \frac{(\delta\Delta_p)^2}{g_p}. \quad (\text{S32})$$

For convenience we will include the f_k in the definition of Δ_p and $\delta\Delta_p$ in this subsection. Evaluating the frequency integral at $T = 0$, taking the trace explicitly, rearranging and keeping only the terms with Ω dependence gives

$$S_2(\Omega) - S_2(\Omega = 0) = - \sum_k \frac{\frac{\Omega^2}{4} \left((\delta\Delta_s)^2 + (\delta\Delta_p)^2 \right) + (\delta\Delta_s\Delta_s + \delta\Delta_p\Delta_p)^2}{2E_k \left(E_k^2 + \frac{\Omega^2}{4} \right)}. \quad (\text{S33})$$

Writing $\sum_k = \nu \int d\xi d\Omega_k$ with Ω_k the angular coordinates on the contours of constant energy, one obtains

$$S_2(\Omega) - S_2(\Omega = 0) = \nu \int d\Omega_k \int d\xi \frac{\frac{\Omega^2}{4} \left((\delta\Delta_s)^2 + (\delta\Delta_p)^2 \right) + (\delta\Delta_s\Delta_s + \delta\Delta_p\Delta_p)^2}{2\sqrt{\xi^2 + \Delta^2} \left(\xi^2 + \Delta^2 + \frac{\Omega^2}{4} \right)}. \quad (\text{S34})$$

Defining $\xi = \Delta \tan x$ we find for the energy integral

$$\frac{1}{2} \int dx \frac{\cos x}{1 + \frac{\Omega^2}{4\Delta^2} \cos^2 x} = \int_0^1 d(\sin x) \frac{1}{1 + \frac{\Omega^2}{4\Delta^2} - \frac{\Omega^2}{4\Delta^2} \sin^2 x} = \frac{1}{2} \frac{\frac{2\Delta}{|\Omega|}}{\sqrt{1 + \frac{\Omega^2}{4\Delta^2}}} \ln \frac{\sqrt{1 + \frac{\Omega^2}{4\Delta^2}} + \frac{|\Omega|}{2\Delta}}{\sqrt{1 + \frac{\Omega^2}{4\Delta^2}} - \frac{|\Omega|}{2\Delta}}. \quad (\text{S35})$$

In the adiabatic limit (lowest order in Ω expansion), the kinetic energy is thus

$$K = \nu \int d\Omega_k \frac{1}{12\Delta^4} \left(3\Delta^2 \left((\partial_t \Delta_s)^2 + (\partial_t \Delta_p)^2 \right) - 2 \left(\Delta_s \partial_t \Delta_s + \Delta_p \partial_t \Delta_p \right)^2 \right) \quad (\text{S36})$$

where $\Delta^2 = \Delta_s^2 + \Delta_p^2$. In 1D, writing $\Delta_s + i\Delta_p = R e^{i\theta}$, the kinetic term becomes

$$K = \frac{\nu}{12R^2} \left((\partial_t R)^2 + 3R^2 (\partial_t \theta)^2 \right). \quad (\text{S37})$$

If Δ_s is very small and the system has a closed Fermi surface in $d = 2$ or $d = 3$ then the adiabatic expansion breaks down in the regions where the gap vanishes. In this case the operator K becomes nonlocal in time, and the physics is most efficiently treated directly from the action Eq. (S2).

1. Dissipative terms

For convenience, we first introduce the general form of correlation functions at zero temperature:

$$\chi_{\sigma_i, \sigma_j}(\omega, q) = \frac{1}{2} \sum_k \frac{1}{\omega^2 - (E_k + E_{k'})^2} \left\{ (E_k + E_{k'}) \text{Tr} \left[\sigma_i \sigma_j - \frac{H_m^k \sigma_i H_m^{k'} \sigma_j}{E_k E_{k'}} \right] + \omega \text{Tr} \left[\frac{\sigma_i H_m^{k'} \sigma_j}{E_{k'}} - \frac{H_m^k \sigma_i \sigma_j}{E_k} \right] \right\} \quad (\text{S38})$$

where $H_m^k = \xi_k \sigma_3 + \Delta_s \sigma_1 + \Delta_p f_k \sigma_2$. We re-derive the kinetic terms by expanding the order parameter correlation functions in frequency:

$$S_2 = \sum_{\omega} \begin{pmatrix} \Delta_s(-\omega) & \Delta_p(-\omega) \end{pmatrix} \begin{pmatrix} \frac{1}{g_s} + \chi_{\Delta_s, \Delta_s}(\omega) & \chi_{\Delta_s, \Delta_p}(\omega) \\ \chi_{\Delta_p, \Delta_s}(\omega) & \frac{1}{g_p} + \chi_{\Delta_p, \Delta_p}(\omega) \end{pmatrix} \begin{pmatrix} \Delta_s(\omega) \\ \Delta_p(\omega) \end{pmatrix} \quad (\text{S39})$$

where the subscripts of the correlation functions correspond to their channels in H_m^k . For example, $\chi_{\Delta_s, \Delta_p} \equiv \chi_{\sigma_1, f_k \sigma_2}$ which is Eq. (S38) with σ_i, σ_j replaced by $\sigma_1, f_k \sigma_2$ everywhere. The Δ_s^2 term in S_2 is

$$\chi_{\Delta_s, \Delta_s}(\omega, 0) = 4 \sum_k \frac{\xi_k^2 + \Delta_p^2 f_k^2}{(\omega^2 - 4E_k^2) E_k} = - \sum_k \frac{1}{E_k} - \int \frac{d\Omega_k}{\Omega_d} (\omega^2 - 4\Delta_s^2) F_0(\Delta_{\Omega_k}, \omega) = \chi_{\Delta_s, \Delta_s}(0, 0) - \omega^2 \nu \begin{cases} \frac{1}{2\Delta_s^2} - \frac{\Delta_s^2}{3\Delta_p^4} & d=1 \\ \frac{\Delta_s^2 + 2\Delta_p^2}{6|\Delta_s|\Delta_p^3} & d=2 \end{cases} + O(\omega^4) \quad (\text{S40})$$

where $\Delta_{\Omega_k}^2 = \Delta_s^2 + \Delta_p^2 f_{k(\Omega_k)}^2$, $\Delta^2 = \Delta_s^2 + \Delta_p^2$, $F_0(\Delta, \omega) = \frac{\nu}{4\Delta^2} \frac{2\Delta}{\omega} \frac{\sin^{-1}(\frac{\omega}{2\Delta})}{\sqrt{1 - (\frac{\omega}{2\Delta})^2}}$ and Ω_k is the angular variable in d -dimension. The Δ_p^2 term is

$$\begin{aligned} \chi_{\Delta_p, \Delta_p}(\omega, 0) &= 4 \sum_k \frac{f_k^2 (\xi_k^2 + \Delta_s^2)}{E_k (\omega^2 - 4E_k^2)} = - \sum_k \frac{f_k^2}{E_k} - \int \frac{d\Omega_k}{\Omega_d} (\omega^2 - 4\Delta_p^2 f_{k(\Omega_k)}^2) F_0(\Delta_{\Omega_k}, \omega) \\ &= \chi_{\Delta_p, \Delta_p}(0, 0) - \omega^2 \nu \begin{cases} \frac{1}{2\Delta_s^2} - \frac{\Delta_p^2}{3\Delta_p^4} & d=1 \\ \frac{1}{6\Delta_p^2} \left[1 - \frac{\Delta_s^2}{\Delta_p^2} \right] & d=2 \end{cases} + O(\omega^4). \end{aligned} \quad (\text{S41})$$

The $\Delta_p \Delta_s$ term is

$$\begin{aligned} \chi_{\Delta_s, \Delta_p}(\omega, 0) &= 4 \sum_k f_k^2 \frac{-\Delta_s \Delta_p}{E_k (\omega^2 - 4E_k^2)} = 4\Delta_s \Delta_p \int \frac{d\Omega_k}{\Omega_d} f_{k(\Omega_k)}^2 F_0(\Delta_{\Omega_k}, \omega) \\ &= \chi_{\Delta_s, \Delta_p}(0, 0) + \omega^2 \nu \begin{cases} \frac{\Delta_s \Delta_p}{3\Delta_p^4} & d=1 \\ \frac{\Delta_s}{3\Delta_p^3} \left[1 - \frac{\Delta_s (2\Delta_s^2 + 3\Delta_p^2)}{2\Delta_p^3} \right] & d=2 \end{cases} + O(\omega^4). \end{aligned} \quad (\text{S42})$$

The above expansions in ω fails as $\omega \sim \Delta_s$, the minimal gap around the fermi surface, especially when $\Delta_s = 0$ such that there are nodes at $k = (0, \pm k_F)$ in 2D. We next evaluate the kernels in the pure p -wave case $\Delta_s = 0$ to gain a rough idea of the crossover of dynamical behavior. The dissipative part of Δ_s kernel is

$$\text{Im}[\chi_{\Delta_s, \Delta_s}(\omega, 0)] = \text{Im} \left[4 \sum_k \frac{E_k}{(\omega + i\eta)^2 - 4E_k^2} \right] = -\pi \sum_k (\delta(\omega - 2E_k) - \delta(\omega + 2E_k)) \xrightarrow{\omega \ll \Delta_p, d=2} -\frac{1}{2} \nu \frac{\omega}{\Delta_p} \quad (\text{S43})$$

where η is an infinitesimal positive number and we have made use of the quasi-particle density of states due to the nodes: $g(E) = \frac{1}{2\pi} k_F E / (v_F \Delta_p)$. The linear in frequency dissipation continues with a cutoff of about Δ_p beyond which it scales as a constant. Kramers-Kronig relation implies that

$$\chi_{\Delta_s, \Delta_s}(\omega, 0) \approx -\frac{1}{2} \nu \left(i \frac{\omega}{\Delta_p} + \frac{\omega^2}{\Delta_p^2} \right). \quad (\text{S44})$$

The dissipative part of Δ_p kernel is

$$\text{Im}[\chi_{\Delta_p, \Delta_p}(\omega, 0)] = \text{Im} \left[4 \sum_k \frac{f_k^2 \xi_k^2}{E_k^2} \frac{E_k}{(\omega + i\eta)^2 - 4E_k^2} \right] = -\pi \sum_k \frac{f_k^2 \xi_k^2}{E_k^2} (\delta(\omega - 2E_k) - \delta(\omega + 2E_k)) \xrightarrow{\omega \ll \Delta_p, d=2} -\frac{\pi}{2^7} \nu \frac{\omega^3}{\Delta_p^3} \quad (\text{S45})$$

and the cubic behavior has the cutoff Δ_p . This together with the $\Delta_s = 0$ limit of Eq. (S41) gives

$$\chi_{\Delta_p, \Delta_p}(\omega, 0) \approx -\frac{\pi}{2^7} \nu \left(i \frac{\omega^3}{\Delta_p^3} + \frac{\omega^2}{6\Delta_p^2} \right). \quad (\text{S46})$$

2. In time domain

With the adiabatic approximation so at time $t_0 + t$ we can write $\Delta(t_0 + t) = \Delta(t_0) + \delta\Delta(t_0 + t)$, the action from Eq. (S31) reads

$$S = \int dt F[\Delta] + \frac{1}{2} \int dt dt' \frac{\partial \delta\Delta}{\partial t} M^R(t - t') \frac{\partial \delta\Delta}{\partial t'} \quad (\text{S47})$$

where M^R is the retarded kernel in time domain as a 2×2 matrix and $\Delta \equiv (\Delta_s, \Delta_p)$ in this subsection. The instantaneous (force) term in the Euler-Lagrange equations comes from the equal time correlator (potential) and the dynamics comes from expanding in derivatives, in other words

$$\frac{\delta F}{\delta \Delta} = \partial_t \int^t dt' M^R(t-t') \partial_{t'} \delta \Delta(t') \quad (\text{S48})$$

Noting that $M^R(0) = 0$ we have

$$\frac{\delta F}{\delta \Delta} = \int^t dt' \partial_t M^R(t-t') \partial_{t'} \delta \Delta(t') \quad (\text{S49})$$

The adiabatic approximation is reasonable if the change in Δ over a time corresponding to the range of M is small ($\partial_t \Delta / |\Delta| \ll 1$) so that we can evaluate M at fixed Δ . If we have a fully gapped configuration (open Fermi surface or Δ_s not small), M decays on times larger than $|\Delta|^{-1} = 1/\sqrt{\Delta_s^2 + \Delta_p^2}$ so we can shift the derivative to the t' and integrate by parts to get

$$\frac{\delta V}{\delta \Delta} = \int^t dt' M^R(t-t') \partial_{t'}^2 \delta \Delta(t') \rightarrow M \partial_t^2 \Delta \quad (\text{S50})$$

with $M = \int^t dt' M^R(t-t')$. However, for closed Fermi surfaces, the vanishing of $\Delta_p f_k$ at some Fermi surface points means that when Δ_s is small M has a part that decays slowly, actually on the time-scale of $1/\Delta_s$ and a more careful analysis is needed. In the isotropic 2D case, we have

$$S_2 = \frac{1}{2} \int dt_1 dt_2 \begin{pmatrix} \partial_t \delta \Delta_s(t_1) & \partial_t \delta \Delta_p(t_1) \end{pmatrix} \mathbf{M}_R(t_1 - t_2) \begin{pmatrix} \partial_t \delta \Delta_s(t_2) \\ \partial_t \delta \Delta_p(t_2) \end{pmatrix} \quad (\text{S51})$$

and the (retarded) correlator is given by

$$\mathbf{M}_R(t) = \Theta(t) \sum_k \frac{\sin 2E_k t}{4E_k^4} \begin{pmatrix} \xi_k^2 + \Delta_p^2 & -\Delta_s \Delta_p f_k \\ -\Delta_s \Delta_p f_k & (\xi_k^2 + \Delta_s^2) f_k^2 \end{pmatrix} \quad (\text{S52})$$

where Θ is the Heaviside step function. Performing the integral over momentum, one obtains the low energy kernel

$$\begin{aligned} \partial_t M_R^{11}(t) &\approx \Theta(t) \frac{v}{2\Delta_p} \int_{\Delta_s}^{\Delta_p} 2dv \left(1 - \frac{\Delta_s^2}{v^2} \right) \cos 2vt + \text{high energy contribution} \\ &= \Theta(t) \frac{v}{2\Delta_p} \left[\frac{\sin 2\Delta_p t - \sin 2\Delta_s t}{t} + \Delta_s \left[2\Delta_s t \left(\frac{\pi}{2} - \text{Si}[2\Delta_s t] \right) - \cos 2\Delta_s t \right] \right] + \frac{v}{6(\Delta_s^2 + \Delta_p^2)} \partial_t \delta(t) \\ &\approx \Theta(t) \frac{v}{2\Delta_p} \frac{\sin 2\Delta_p t - \sin 2\Delta_s t}{t} + \frac{v}{6(\Delta_s^2 + \Delta_p^2)} \partial_t \delta(t), \\ \partial_t M_R^{22}(t) &\approx \frac{v}{6(\Delta_s^2 + \Delta_p^2)} \partial_t \delta(t) \end{aligned} \quad (\text{S53})$$

The off diagonal terms don't affect the qualitative dynamics which we neglect. At small Δ_s we can neglect the second term of $\partial_t M_R^{11}$. Therefore, in 2D, a smooth crossover between non dissipative and dissipative behaviors during the swiping across $\theta = \pi/2$ can be described by the retarded Kinetic kernel

$$S_{\text{dis}} = \frac{1}{2} \int dt dt' \dot{\Delta}_s(t) M_R(t-t') \dot{\Delta}_s(t'), \quad M_R(t) \approx \frac{v}{2|\Delta_p|} \int_0^t dt' \frac{\sin 2\Delta_p t' - \sin 2\Delta_s t'}{t'}. \quad (\text{S54})$$

Eq. (S54) implies the equation of motion

$$\frac{\delta F}{\delta \Delta_i} = \frac{v}{6(\Delta_s^2 + \Delta_p^2)} \partial_t^2 \Delta_i + \frac{v \delta i, s}{2\Delta_p} \int_{-\infty}^t dt' \frac{\sin [2\Delta_p(t-t')] - \sin [2\Delta_s(t-t')]}{t-t'} \Delta_i(t') \quad (\text{S55})$$

which describes the dissipationless-dissipative crossover behavior when Δ_s crosses zero during the dynamics.

C. The drive term

In the drive term $L_{\text{drive}} = -P(\theta)E - s(\Delta_s, \Delta_p)E^2 + O(E^3)$, the linear coupling of electric field to the polarization is obvious. We derive the second term in this section. The kernel of the $O(A^2)$ term is [33]

$$K_{ij}(\omega) = \left(\frac{n}{m} + \chi_{J_i, J_j}(\omega) \right) \delta_{ij} \quad (\text{S56})$$

where J is the current operator in Eq. (S6) and m is the electron mass in our model. Since the second term in the current in Eq. (S6) is suppressed by the factor Δ_p/ε_F in the BCS limit, its contribution can be neglected. In 1D, the current correlation function is thus

$$\chi_{J, J}(\omega) = \chi_{\sigma_3 v_k, \sigma_3 v_k}(\omega) = -4v_F^2 \Delta^2 F_0(\Delta, \omega) = -v_F^2 v \left(1 + \frac{2}{3} \left(\frac{\omega}{2\Delta} \right)^2 + O\left(\left(\frac{\omega}{2\Delta} \right)^4 \right) \right) \quad (\text{S57})$$

where $\Delta^2 = \Delta_s^2 + \Delta_p^2$ and $F_0(\omega) = \sum_k \frac{1}{E_k(4E_k^2 - \omega^2)} = \frac{v}{4\Delta^2} \frac{2\Delta}{\omega} \frac{\sin^{-1}(\frac{\omega}{2\Delta})}{\sqrt{1 - (\frac{\omega}{2\Delta})^2}} = \frac{v}{4\Delta^2} \left(1 + \frac{2}{3} \left(\frac{\omega}{2\Delta} \right)^2 + O\left(\left(\frac{\omega}{2\Delta} \right)^4 \right) \right)$. The constant term cancels the diamagnetic contribution n/m and what remains in the kernel is the $O(\omega^2)$ term that corresponds to the static polarizability from ‘scattering states’ of the electron hole pair. In 2D, the current correlator up to $O(\omega^2)$ is

$$\chi_{J_i, J_j}(\omega) = -\delta_{ij} \frac{1}{d} v_F^2 v \int \frac{d\theta_k}{2\pi} \left(1 + \frac{2\cos^2 \theta_k}{3} \frac{\omega^2}{4(\Delta_s^2 + \Delta_p^2 \cos^2 \theta_k)} \right) = -\delta_{ij} \frac{1}{d} v_F^2 v \left(1 + \frac{1}{6} \frac{\omega^2}{\Delta_s^2 + \Delta_p^2 + |\Delta_s| \sqrt{\Delta_s^2 + \Delta_p^2}} \right). \quad (\text{S58})$$

Therefore, the $O(E^2)$ term in the action reads

$$L_2 = \frac{1}{\omega^2} K_{ij} E_i E_j = -\frac{1}{6} v \Delta^2 \left(\frac{E}{E_0} \right)^2 \begin{cases} \frac{\Delta^2}{\Delta_s^2 + \Delta_p^2} & d = 1 \\ \frac{\Delta^2}{\Delta_s^2 + \Delta_p^2 + |\Delta_s| \sqrt{\Delta_s^2 + \Delta_p^2}} & d = 2 \end{cases} \quad (\text{S59})$$

where the coefficient can be interpreted as $s = \lim_{\omega \rightarrow 0} \sigma(\omega)/(2i\omega)$. The higher order terms in E are in higher powers of $\left(\frac{E}{E_0} \right)^2 \frac{\Delta^2}{\Delta_s^2 + \Delta_p^2}$ where E_0 is defined in the main text.

V. THE ADIABATIC TRANSPORT SCHEME

A. Description

If the sin pulse is wide enough in time, it is possible to make the dynamics perfectly adiabatic since the system simply follows the instantaneous minimum on the free energy landscape. As the field increases, the minimum shifts away from $(\Delta, 0)$ counter clockwise while the maximum at $(0, \Delta_{p0})$ shifts clockwise. The maximum field needed is simply that making the instantaneous minimum and maximum coincide. In 1D, this field can be computed analytically:

$$E_m(g_p) = 2t\sqrt{1-x^2}e^{-1/2-t+\sqrt{t^2+1/4}} \quad (\text{S60})$$

where $x = (-1/t + \sqrt{1/t^2 + 4})/2$ and $t = 1/(vg_p) - 1/(vg_s)$. After reaching the maximum value (a little higher than that), the field starts to decrease, shifting back the two extrema. The order parameter is moved to the immediate left of the maximum, which gradually shifts back to $(0, \Delta_{p0})$ as the field decreases to zero. The second half of the sin pulse would therefore transport the order parameter to the minimum at $(-\Delta, 0)$, completing a half cycle. However, if the decreasing field phase of the pulse is too slow, unstable fluctuations of order parameter tend to grow exponentially[8] and get comparable to its mean field value within the ‘spinodal time’ $\frac{1}{|\Delta|} \ln \frac{1}{G_0}$ where $G_0 \sim \frac{|\Delta|}{\varepsilon_F} \ll 1$ is the Ginzburg parameter of the Landau theory. Therefore, the time scale of the pulse has to be smaller than the spinodal time.

If g_p is too small, the required maximum field is so large that the $O(E^2)$ term $L_2 = -\frac{1}{6} v \frac{E^2}{E_0^2} \frac{\Delta^4}{\Delta_s^2 + \Delta_p^2}$ would pull the order parameter to the origin and destroy the above adiabatic trajectory. This imposes an lower bound for the p -wave pairing strength $g_{pc} = g_s/(1 + \sqrt{3/8}vg_s)$. For the adiabatic transport scheme to work, g_p has to be larger than g_{pc} . These conclusions apply qualitatively to higher dimensions.

If the adiabatic scheme is realized, experimental measurement of the threshold electric field gives the estimation of g_p through Eq. (S60). In the fast scheme described in the main text, if the full frequency spectrum of the current can be measured, it is possible to reconstruct the angular dynamics through, e.g., Eq. (6) of the main text.

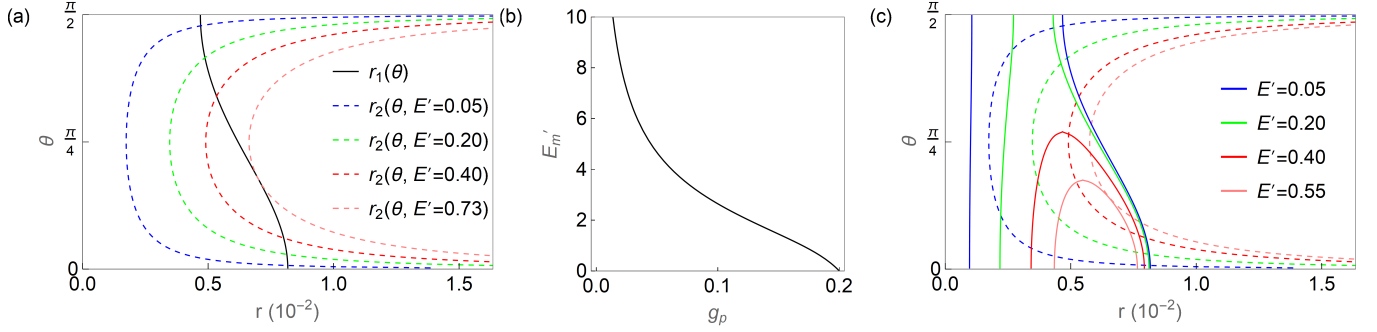


FIG. S3. (a) The curves r_1 and r_2 on the (r, θ) plane at various values of electric field E' , neglecting $O(E^2)$ terms in the free energy. Solid curves are r_1 and dashed curves are r_2 . The intersections between the solid black curve and the dashed curves are the saddle points. The parameters are $g_s = 0.2$ and $g_p = 0.18$. (b) The maximum field E_m as a function of g_p for $g_s = 0.2$. (c) Same as (a) but with the $O(E^2)$ terms taken into account. The r_2 curves are not affected by the $O(E^2)$ terms while r_1 curves are deformed. Each r_1 curve can be separated into two branches: the left branch has $\partial_r^2 f < 0$ (maxima) while the right branch has $\partial_r^2 f > 0$ (minima).

B. Derivation

In 1D, incorporating the effect of a static electric field up to $O(E^2)$, the free energy is

$$f(\Delta_s, \Delta_p) = v \left(-r^2 \ln \frac{2\Lambda}{r} + \frac{1}{v g_s} r^2 + \left(\frac{1}{v g_p} - \frac{1}{v g_s} \right) r^2 \sin^2 \theta - \frac{1}{2} \Delta_0^2 E' \theta - \frac{1}{6} E'^2 \frac{\Delta_0^4}{r^2} \right) \quad (\text{S61})$$

where the ‘polar’ coordinate is defined as $(\Delta_s, \Delta_p) = r(\cos \theta, \sin \theta)$, the dimensionless electric field is $E' = E/E_0$, $E_0 = \Delta_0^2 / v_F$ and $\Delta_0 = \Delta$. Note that r is R in the main text. We look for saddle points on the free energy landscape within the domain $\theta \in [0, \pi/2]$. There are two curves defined by $\partial_r f = 0$ and $\partial_\theta f = 0$ respectively, whose solutions read

$$r_1(\theta) = \Lambda e^{-\frac{1}{g_s v} - t \sin^2 \theta - \frac{1}{2}}, \quad r_2(\theta) = \sqrt{\frac{1}{2t} \frac{\Delta_0^2 E'}{\sin 2\theta}} \quad (\text{S62})$$

where $t = \frac{1}{v g_p} - \frac{1}{v g_s}$, as shown in Fig. S3(a). Note that we temporarily neglected the $O(E^2)$ terms in the free energy. The intersections of the two curves are the saddle points. At zero field, the two saddle point are just the two minima at $(\theta, r) = (0, \Delta_0), (\pi/2, \Delta_{p0})$. For weak field, the two saddle points shift towards each other in angular direction. As the field further increases to the critical value E_m , the two saddle point meet which means the two lines are tangent to each other: $r_1 = r_2, \partial_\theta r_1 = \partial_\theta r_2$ is satisfied at the intersection. This condition gives the angle at intersection as $\cos(2\theta_m) = \frac{1}{2} \left(-\frac{1}{t} + \sqrt{\frac{1}{t^2} + 4} \right)$ and critical field

$$E'_m = 2t \sin(2\theta_m) e^{-1/2 - t + \sqrt{t^2 + 1/4}}. \quad (\text{S63})$$

It increases from zero as g_p decreases from g_s , and diverges as $1/\sqrt{g_p}$ as $g_p \rightarrow 0$, as shown in Fig. S3(b).

The $O(E^2)$ term in Eq. (S61) lowers the energy dramatically close to $r = 0$, and therefore tends to pull the system to the zero order state. As a result, the free energy has a maximum in the r direction, followed by the minimum as r increases. Thus the r_1 curve has two branches: the left one has $\partial_r^2 f < 0$ (maxima) while the right one has $\partial_r^2 f > 0$ (minima), as shown by the solid curves in Fig. S3(c) for weak fields. For strong enough field E , it can happen that the two branches meet each other at certain $\theta(E)$ such that there will be no saddle points along r if $\theta > \theta(E)$, as shown by the solid curves in Fig. S3(c) for stronger fields. The summits of those curves satisfy $(\partial_r, \partial_r^2) f = (0, 0)$ which yields

$$E' = \frac{3}{2} \frac{r^4}{\Delta_0^4}, \quad r = 2\Lambda e^{-\left(\frac{1}{v g_s} + t \sin^2 \theta\right) - \frac{3}{4}}. \quad (\text{S64})$$

Making the summit at $\theta = \pi/2$, the pure p -wave order line, one obtains the minimal field $E'_c = \sqrt{3/2} e^{-2t - 1/2}$ for the r_1 curves to be closed, i.e., for the minima in r direction to disappear at certain angles.

As the field increases, the intersections A, B between the r_2 curve and the right branch of r_1 curve moves towards each other. If they successfully meet each other at certain field E_m , the order parameter is handed by B to A and the subsequent decreasing field phase pushes A back to the p -wave order, i.e., adiabatic transport works. However, if g_p is too weak, it

can happen that A annihilates with another intersection on the left branch of r_1 . In this situation, the order parameter will be transported to zero order instead of to the p -wave state. The critical p -wave pairing strength can be estimated roughly in this way: the summit of r_1 collides with the left most point of r_2 as field increases. This condition leads to the equality $r^2 = \sqrt{2/3}\Delta_0^2 E' = \frac{1}{2t}\Delta_0^2 E'$ which renders $g_{pc} = g_s/(1 + \sqrt{3/8}v g_s)$.

VI. EXACT MEAN FIELD DYNAMICS

A. Pseudo spin representation

The degree of freedom at each momentum k in Eq. (2) of the main text can be mapped to an Anderson pseudo spin \mathbf{s}_k . In the second quantized language, each momentum k labels two single particle states from the two bands whose annihilation operators are $\psi_{c,k}$ and $\psi_{v,k}$, giving a 4-dimensional Hilbert space. However, the mean field dynamics here implies that the total occupation number $n_k = \psi_{c,k}^\dagger \psi_{c,k} + \psi_{v,k}^\dagger \psi_{v,k} = \psi_k^\dagger \sigma_0 \psi_k$ at k is always one (n_k commutes with the Hamiltonian) where $\psi_k^\dagger = (\psi_{c,k}^\dagger, \psi_{v,k}^\dagger)$ and σ_0 is the identity matrix. Therefore, it is enough to consider a 2-dimensional subspace of single occupancy which can be mapped to a pseudo spin-1/2 defined as $\hat{\mathbf{s}}_k \equiv \psi_k^\dagger \boldsymbol{\sigma} \psi_k$ where $\boldsymbol{\sigma}$ are the three Pauli matrices.

The general mean field Hamiltonian at momentum k can be written as

$$\psi_k^\dagger H_m^k \psi_k = \psi_k^\dagger \begin{pmatrix} \xi_k & \Delta_s - i\Delta_p f_k \\ \Delta_s^* + i\Delta_p^* f_k & -\xi_k \end{pmatrix} \psi_k = \mathbf{b}_k \cdot \hat{\mathbf{s}}_k \quad (\text{S65})$$

and the dynamics implied by Eq. (1) of the main text is mapped to the procession of the Anderson pseudo spins $\mathbf{s}_k = \langle \hat{\mathbf{s}}_k \rangle$ in the time dependent self consistent mean field \mathbf{b}_k [46]:

$$\dot{\mathbf{s}}_k = (\mathbf{b}_k - \gamma \mathbf{b}_k \times \mathbf{s}_k) \times \mathbf{s}_k,$$

$$\mathbf{b}_k = (\text{Re}[\Delta_s] + \text{Im}[\Delta_p] f_k, -\text{Im}[\Delta_s] + \text{Re}[\Delta_p] f_k, \xi_k) = \left(\frac{g_s}{2} \sum_{k'} s_{1k'} + \frac{g_p}{2} f_k \sum_{k'} f_{k'} s_{1k'}, \frac{g_s}{2} \sum_{k'} s_{2k'} + \frac{g_p}{2} f_k \sum_{k'} f_{k'} s_{2k'}, \xi_k \right) \quad (\text{S66})$$

where the last equality is known as the gap equation. The EM vector potential $A(t)$ enters by $k \rightarrow k - A(t)$ and we use a phenomenological damping γ to account for the effect of energy loss due to, e.g., the phonon bath. Starting with the ground state with a real Δ_s , we simulated the dynamics induced by a pulse and the current $j_i = \sum_k \mathbf{s}_k \cdot \partial_{k_i} \mathbf{b}_k$ is integrated over time to obtain the pumped charge. Some numerical solutions to Eq. (S66) are shown in Figs. S5 and S6.

Note that Eqs. (S65) and (S66) are general which allows for appearance of imaginary components of Δ_s and Δ_p . However, as a result of an emergent ‘particle-hole’ symmetry in the BCS weak coupling case that maps (Δ_s, Δ_p) to (Δ_s^*, Δ_p^*) , the order parameter dynamics is restricted to the $s + ip$ plane where $\Delta_s(t), \Delta_p(t)$ are always real numbers which we prove in the next subsection. Away from BCS weak coupling, the order parameter trajectory departs from the $s + ip$ plane in a continuous way: e.g., Δ_p can temporarily develop an imaginary component that couples to σ_1 and Δ_s can have an imaginary component that couples to σ_2 . However, since the initial and final states are the same ones, and the charge pumping is still quantized for 1D systems because it is a topological effect.

1. Proof of why the dynamics is confined within the $s + ip$ plane in the BCS weak coupling case

The physical argument is that in the BCS weak coupling case, there will be no force pushing the order parameter away from the $s + ip$ plane during the dynamics. Following we provide a more mathematical proof. Define the ‘particle-hole’ operation

$$\hat{P}_h: (\psi_{c,\mathbf{k}}, \psi_{v,\mathbf{k}}) \rightarrow (\psi_{v,\mathbf{k}'}, \psi_{c,\mathbf{k}'}), \quad \Delta_{\mathbf{k}} \rightarrow \Delta_{\mathbf{k}}^*, \quad \mathbf{k}' = \mathbf{k} - 2k_F \hat{\mathbf{k}} \quad (\text{S67})$$

where k_F is the magnitude of Fermi momentum, $\hat{\mathbf{k}}$ is the unit vector along the direction of \mathbf{k} and we have used bold fonts for the momentum to emphasize its vector nature (although every k in the main text and supplemental material already means a vector). The operation \hat{P}_h changes \mathbf{k} to its ‘particle-hole’ image \mathbf{k}' , as illustrated in Fig. S4. In the BCS weak coupling case ($|\Delta_s|, |\Delta_p| \ll G$), what is relevant are the low energy states close to the Fermi surface (band crossing point) where \hat{P}_h becomes a symmetry of the action in Eq. (1) of the main text (note that $\xi_{\mathbf{k}} = -\xi_{\mathbf{k}'}$). Considering that $f_{\mathbf{k}'} = -f_{\mathbf{k}}$ in the BCS weak coupling case, (Δ_s, Δ_p) is changed to its complex conjugate (Δ_s^*, Δ_p^*) under operation of \hat{P}_h according to Eq. (S67) and Eq. (S65). Therefore, given a solution $(\Delta_s(t), \Delta_p(t))$ to the order parameter dynamics, its ‘image’ $(\Delta_s^*(t), \Delta_p^*(t))$ must also be a solution. Given the initial condition of $(\Delta_s(0), \Delta_p(0)) = (|\Delta|, 0)$, since the solution is unique, the order parameter trajectory must lie within the plane of $\Delta_s, \Delta_p \in \mathbb{R}$, i.e., the $s + ip$ plane studied in the main text.

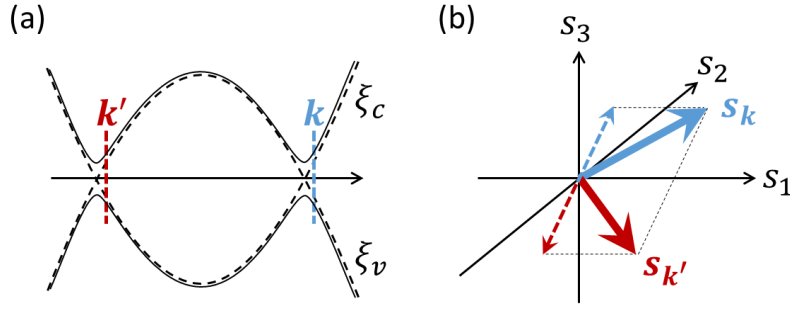


FIG. S4. (a) Illustration of the momentum \mathbf{k} and its ‘particle hole’ image \mathbf{k}' on the diagram of quasi particle energy dispersion as a function of momentum. (b) Solid arrows are the pseudo spins $\mathbf{s}_{\mathbf{k}}$ and $\mathbf{s}_{\mathbf{k}'}$ in the 1-2-3 space. Dashed arrows are their projections on the 2-3 plane.

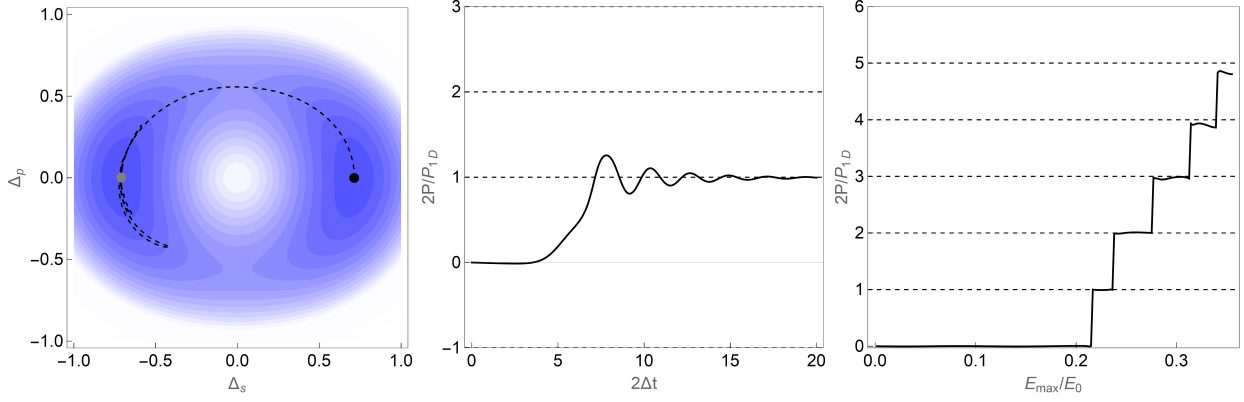


FIG. S5. Order parameter dynamics of an 1D excitonic insulator subject to a pump pulse described by the vector potential $A(t) = -E_{\max}w \left(\tanh\left(\frac{t-t_0}{w}\right) + 1 \right)$. Left panel is the trajectory on the free energy landscape plotted on the $s + ip$ plane for $E_{\max} = 0.22E_0$. Middle panel is the polarization as a function of time. Right panel is the pumped charge as a function of E_{\max} . The parameters are $w = 1/(2\Delta)$, $g_s v = 0.3$, $g_p v = 0.28$, $\Delta = 2\Lambda e^{-1/(g_s v)} = 0.071\Lambda$, $\gamma = 0.07\Delta$, $E_{\max} = 0.22E_0$. The grid in time direction is 10^4 .

An alternative way to prove this is using the pseudo-spin language. According to Eq. (S66), to prove that $(\Delta_s(t), \Delta_p(t))$ is always real, we just need to prove $\mathbf{s}_{\mathbf{k}}$ and $\mathbf{s}_{\mathbf{k}'}$ are always related to each other by the ‘mirror’ operation \hat{M} with respect to ‘2–3’ plane: $(s_1, s_2, s_3)_{\mathbf{k}} = (s_1, -s_2, -s_3)_{\mathbf{k}'}$, as shown in Fig. S4(b). Note that the pseudo spins are defined as axial vectors such that the mirror operation $\hat{M} = \hat{s}_1$ transforms the spins as $(s_1, s_2, s_3) \rightarrow (s_1, -s_2, -s_3)$. For the initial ground state, this is obviously true and the ‘magnetic field’ $\mathbf{b}_{\mathbf{k}/\mathbf{k}'}$ on the two pseudo-spins are also mirror images of each other under M , so are $(\mathbf{b} \times \mathbf{s})_{\mathbf{k}/\mathbf{k}'}$. Therefore, this ‘mirror’ relation between the pseudo spins at \mathbf{k}/\mathbf{k}' is sustainable during the dynamics according to Eq. (S66), and guarantees that the order parameter stays on the $s + ip$ plane.

B. ‘Super-current’ in 1D systems

The solution is trivial in the degenerate case $g_s = g_p$ in the BCS limit where the effect of the pairing function f_k is captured by $f_{\pm k_F} = \pm 1$ on the right/left fermi point. We start from a ground state $(\Delta_s, \Delta_p) = (\Delta, 0)$ where all spins are pointing in 1–3 plane: $\mathbf{s}_{\mathbf{k}} = (\Delta, 0, \xi_k)/E_k$. Consider the electric field pulse at $t = 0$ applied through $A = A_0\Theta(t)$. The leading driving term due to electric field is $\mathbf{b}_{\mathbf{k}} = (0, 0, v_k A)$ where $v_k = \pm v_F$ around the right/left fermi point. The diamagnetic term $\sim A^2$ is subleading in driving the spinor dynamics but contributes a diamagnetic current we will discuss in the end. After the kick, the spinors start to rotate around the ‘3’ axis with angular frequency $\omega = 2v_F A_0$. The mean field rotates at the same speed: $(\Delta_s, \Delta_p) = \Delta(\cos(\omega t), \sin(\omega t))$ such that $\mathbf{b}_{\mathbf{k}} - (0, 0, v_k A)$ is always parallel to each spinor, not affecting the spin rotation. Thus the solution is that each spin synchronize and keeps rotating around ‘3’ with angular frequency $v_F A_0$. Now we evaluate the current $J = J_P + J_D$. The paramagnetic current $J_P = \sum_k \langle v_k \sigma_3 \rangle$ vanishes in this state. The diamagnetic current is $j_D = \frac{2}{\pi} v_F A_0 = 2\omega/(2\pi)$. Therefore, the system behaves like a ‘superconductor’ with the superfluid density n .

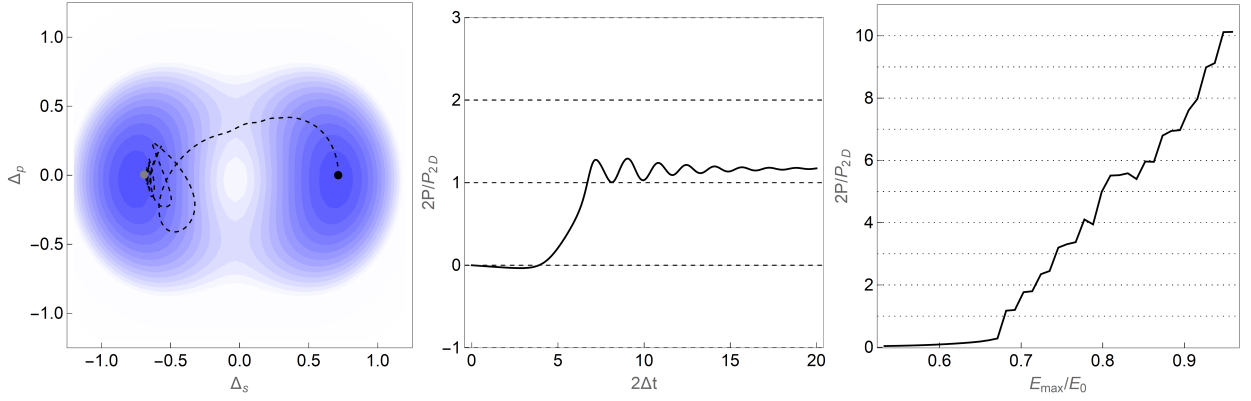


FIG. S6. Order parameter dynamics of a 2D excitonic insulator subject to a pump pulse described by the vector potential $A(t) = -E_{\max} w \left(\tanh\left(\frac{t-t_0}{w}\right) + 1 \right)$. Left panel is the trajectory on the free energy landscape plotted on the $s + ip$ plane for $E_{\max} = 0.686E_0$. Middle panel is the polarization as a function of time. Right panel is the pumped charge as a function of E_{\max} . The parameters are $w = 1/(2\Delta)$, $g_s v = 0.3$, $g_p v = 0.5$, $\Delta = 2\Lambda e^{-1/(g_s v)} = 0.071\Lambda$, $\gamma = 0.07\Delta$. The grid in time direction is 10^4 . Here the p -wave pairing interaction g_p is weaker than Fig. 4 of the main text, so that stronger field is needed to induce the dynamics and the nonadiabatic correction to polarization is larger.

C. Dynamics of the node in 2D: Landau-Zener formula

The node contribution to the polarization is captured by a Dirac Hamiltonian with time dependent gap:

$$H_k(t) = \frac{\Delta_p}{k_F v_F} v_F k_x \sigma_2 + v_F k_y \sigma_3 + \Delta_s(t) \sigma_1 \quad (\text{S68})$$

which is an approximation to Eq. (2) of the main text around $k_0 = (0, k_F)$, and is valid for $k_x, k_y \ll k_F$. Taking into account the higher order term $\frac{k_x^2}{2m} \sigma_3$ in the Hamiltonian, the current in x direction is $J_x = \frac{v_F}{k_F} k_x \sigma_3 + \frac{\Delta_p}{k_F} \sigma_2$. In the BCS limit we are concerned here, during the dynamics, the spinor at (k_x, k_y) is always the mirror image (under \hat{M} defined in Sec. VI) of that at $(-k_x, -k_y)$ with respect to the 2–3 plane. Therefore, the σ_2 contributions to the current will always sum to zero, and it is enough to consider $J_x = \frac{v_F}{k_F} k_x \sigma_3$. Define the energy variables $k'_x = \frac{\Delta_p}{k_F} k_x$, $k'_y = v_F k_y$, the Hamiltonian becomes

$$H_k(t) = k'_x \sigma_2 + k'_y \sigma_3 + \Delta_s(t) \sigma_1 \quad (\text{S69})$$

and the current reads $J_x = \frac{v_F}{\Delta_p} k'_x \sigma_3$. We now use Eq. (S69) to study the spinor dynamics and the current generated.

As the order parameter passes the $(0, \Delta_p)$ point with nearly constant velocity, the nodal gap Δ_s changes sign. For the spinor at certain k , as Δ_s swipes from the positive value Δ at time $-t_0$ to negative value $-\Delta$ at time t_0 , the energy splitting starts from $\sqrt{\delta_k^2 + \Delta^2}$, passes through the minimal splitting $|\delta_k| = |k'|$, and ends up with $\sqrt{\delta_k^2 + \Delta^2}$. If the initial state is the low energy state, the probability of finally tunneling into the high energy state is given by the Landau-Zener formula [45]:

$$P_k = e^{-2\pi \frac{\delta_k^2}{|\partial_t \Delta_s|}} \quad (\text{S70})$$

which is exact if $\Delta \gg \delta_k$. Therefore, the tunneling probability is unity at the node and decays to zero away from the node within a range of $\sim \sqrt{|\partial_t \Delta_s|}$. Considering there are two nodes, the total number of quasiparticles excited is thus

$$N = 2 \sum_k P_k = \frac{2}{4\pi^2} \frac{k_F}{v_F \Delta_p} \int dk'_x dk'_y e^{-\pi \frac{k'^2}{|\partial_t \Delta_s|}} = \frac{2}{4\pi^2} \frac{k_F}{v_F \Delta_p} \pi \frac{|\partial_t \Delta_s|}{\pi} = \frac{1}{2\pi^2} \frac{k_F}{v_F} \frac{|\partial_t \Delta_s|}{\Delta_p} = \frac{k_F^2}{2\pi^2} \frac{1}{k_F v_F} \frac{|\partial_t \Delta_s|}{\Delta_p}. \quad (\text{S71})$$

Since we have assumed Dirac dispersion in the integral, Eq. (S71) is accurate if $\sqrt{|\partial_t \Delta_s|} \ll \Delta_p$.

1. The pumped charge around the node

We now compute the pumped charge, which reads

$$P = 2 \sum_k \int dt \langle J_x(k) \rangle_t = \frac{2}{4\pi^2} \frac{k_F}{\Delta_p^2} \int dk'_x dk'_y dt k'_x \langle \sigma_3 \rangle_{k,t} = P_0 + P_{dis}. \quad (S72)$$

The integral is completely determined by the dynamics governed by Eq. (S69), the evaluation of which requires more detailed analysis of the time evolution of each spinor. Before that, we can guess the result simply from dimensional analysis. The nonadiabatic correction P_{dis} comes from spinors with $\delta_k \ll \Delta$, and the contribution arises during the anti crossing time regime when $\Delta_s(t)$ is not much larger than δ_k . Therefore, neither the momentum cutoff nor the maximum value of Δ_s should enter the result. The only remaining energy scale in Eq. (S69) is provide by $\partial_t \Delta_s$ which has the unit of energy squared. Since the integral in P_{dis} has the unit of energy squared, one obtains $P_{dis} = \kappa \frac{k_F}{2\pi^2} \frac{|\partial_t \Delta_s|}{\Delta_p^2}$ where κ is a universal $O(1)$ constant.

Now we compute P_{dis} exactly. It is more convenient to perform a permutation of the Pauli matrices: $(\sigma_2, \sigma_3, \sigma_1) \rightarrow (\sigma_1, \sigma_2, \sigma_3)$ such that the node Hamiltonian reads

$$H_k(t) = k'_x \sigma_1 + k'_y \sigma_2 + \Delta_s(t) \sigma_3 \quad (S73)$$

and the current becomes $J_x = \frac{v_F}{\Delta_p} k'_x \sigma_2$. The dynamics of the pseudo spin at k' is a Landau-Zener problem [45]. At time $-t_0$, we have $\Delta_s = \Delta \gg k'$ and the spin is in the ground state: $\psi = (0, 1)^T$. The time evolution can be written as $\psi = (A(t)e^{-i\phi(t)}, B(t)e^{i\phi(t)})^T$ where $\phi(t) = \int dt \Delta_s(t)$ should not be confused with that from Sec. II. The Schrodinger equation for the amplitudes reads

$$\partial_t A = -i(k'_x - ik'_y)B e^{i\phi}, \quad \partial_t B = -i(k'_x + ik'_y)A e^{-i\phi} \quad (S74)$$

which leads to

$$\partial_t^2 A - i2\Delta_s(t)\partial_t A + k'^2 A = 0, \quad \partial_t^2 B + i2\Delta_s(t)\partial_t B + k'^2 B = 0. \quad (S75)$$

The current involves the expectation value of σ_2 :

$$\langle \sigma_2 \rangle = i \left(B^* A e^{i\theta} - c.c. \right) = - \left(\frac{1}{k'_x - ik'_y} B \partial_t B^* + c.c. \right) \quad (S76)$$

whose time integral gives the charge:

$$\int dt \langle \sigma_2 \rangle = -\text{Re} \left[\frac{1}{k'_x - ik'_y} \right] (|B(t_0)|^2 - |B(-t_0)|^2) - i \text{Im} \left[\frac{1}{k'_x - ik'_y} \right] \int dt |B(t)|^2 \partial_t \ln \left(\frac{B^*}{B} \right). \quad (S77)$$

It can be seen from Eq. (S75) that the time dependent wave function is the same between the spins at (k'_x, k'_y) and $(-k'_x, k'_y)$. Since the current is $j_x = \frac{v_F}{\Delta_p} k'_x \sigma_2$, the second term in Eq. (S77) will be canceled out by the two spins. The first term just needs the initial and final state information:

$$\int dt \langle \sigma_2 \rangle = -\text{Re} \left[\frac{1}{k'_x - ik'_y} \right] (|B(t_0)|^2 - |B(-t_0)|^2) = \text{Re} \left[\frac{1}{k'_x - ik'_y} \right] (1 - P_k). \quad (S78)$$

which is provide by the Landau-Zener formula. Summing over all the spins, the pumped charge reads

$$P = \frac{2}{4\pi^2} \frac{k_F}{\Delta_p^2} \int dk'_x dk'_y k'_x \text{Re} \left[\frac{1}{k'_x - ik'_y} \right] (1 - P_k) = P_0 + P_{dis} \quad (S79)$$

where the nonadiabatic correction is identified as

$$\begin{aligned} P_{dis} &= -\frac{2}{4\pi^2} \frac{k_F}{\Delta_p^2} \int dk'_x dk'_y k'_x \text{Re} \left[\frac{1}{k'_x - ik'_y} \right] P_k \\ &= -\frac{2}{4\pi^2} \frac{k_F}{\Delta_p^2} \int dk'_x dk'_y \frac{k_x^2}{k^2} e^{-\pi \frac{k'^2}{|\partial_t \Delta_s|}} = -\frac{2}{4\pi^2} \frac{k_F}{\Delta_p^2} \int dk' d\theta k' \cos^2 \theta e^{-\pi \frac{k'^2}{|\partial_t \Delta_s|}} = -\frac{k_F}{8\pi^3} \frac{|\partial_t \Delta_s|}{\Delta_p^2}. \end{aligned} \quad (S80)$$

Due to the negative relative sign of the non-adiabatic correction to the adiabatic one, we conclude that

$$P_{dis} = -\frac{k_F}{8\pi^3} \frac{|\partial_t \Delta_s|}{\Delta_p^2} = -P_0 \frac{1}{8\pi^2} \frac{|\partial_t \Delta_s|}{\Delta_p^2}. \quad (\text{S81})$$

Therefore, Eq. (S81) gives the non adiabatic correction during each half cycle of order parameter rotation, which is valid if $\sqrt{|\partial_t \Delta_s|} \ll \Delta_p$. This formula is nonperturbative in the swiping speed in the sense that, it can not be obtained by integrating over instantaneous linear or nonlinear current response functions perturbatively over the time evolution.